Spring 2021

Plasmids Bring Novel Functions to *Caulobacter* Genomes

Taylor Howell Carter

PLASMIDS BRING NOVEL FUNCTIONS TO *CAULOBACTER* GENOMES

by

Taylor Howell Carter

Bachelor of Arts
University of South Carolina, 2012

Submitted in Partial Fulfillment of the Requirements

For the Degree of Doctor of Philosophy in

Biological Sciences

College of Arts and Sciences

University of South Carolina

2021

Accepted by:

Bert Ely, Major Professor

Rekha Patel, Committee Chair

Daniel Speiser, Committee Member

Jason Stewart, Committee Member

Thomas Makris, Committee Member

Tracey L. Weldon, Interim Vice Provost and Dean of the Graduate School

DEDICATION

This is dedicated to Chester Ray Carter, Casey Burke, Kevin Garczynski and Jeremy Pilzer. The ones who always believed I would make it this far but are not able to witness it.

ACKNOWLEDGEMENTS

First and foremost, I would like to thank Dr. Bert Ely for giving me this opportunity to complete my PhD. I would like to thank my Mom, Judith Carter, for always being there. I would like thank Dr. Erin Puro for her assistance in allowing me to work through PTSD. I would like to thank Pastor Jeff Donaldson for strengthening my relationship with God while not having to put aside my scientific beliefs. Finally, I would like to thank Eva Zaragoza for her calming presence in the final years of my graduate work.

ABSTRACT

Caulobacter is a well-studied bacterial genus, but little is known about the plasmids that are found in some wild *Caulobacter* isolates. We identified nine plasmids from seven different *Caulobacter* strains and grouped them based on their size and the similarity of their *repABC*, *parAB*, and *mobAB* genes. Protein pathway analysis of the genes on the K31p1, and K31p2 plasmids showed many metabolic pathways that would enhance the metabolic versatility of the host strain. In contrast, the CB4 plasmid contained 21 heavy metal resistance genes organized into 9 operons. The majority of the CB4 heavy metal resistance genes code for genes that enhance copper resistance. Growth assays demonstrated increased copper resistance and quantitative PCR showed an increase in the expression of eight of the nine heavy metal operons when induced with copper.

TABLE OF CONTENTS

LIST OF TABLES

LIST OF FIGURES

CHAPTER 1

INTRODUCTION

Heavy metal poisoning is an ongoing threat to many ecosystems across the planet due to increased pollution levels. As more toxic waste is released into the environment, heavy metal levels will continue to rise. Plants are under a particular threat since they have no ability to move to another habitat if theirs becomes polluted. On the other hand, some plants can accumulate heavy metals, and they can be used to remove heavy metals from a polluted environment (1). Bacteria within the *Caulobacter* genus have been shown to have plant growth promoting activity, heavy metal resistance, and the ability to colonize mineral rich soil (2,3). This combination of plant growth promotion and heavy metal resistance could potentially benefit plants in polluted environments. The heavy metal resistance and ability to colonize mineral rich soil could benefit soil conservation projects as well.

Caulobacter crescentus is a well-studied (4) Alphaproteobacterium with a di-morphic life cycle (5). This unique life cycle combines a motile swarmer cell with a nonmotile stalked cell, with DNA replication only occurring in the nonmotile stalked cell (6). As a result, *C. crescentus* has been an excellent model system for the study of cellular differentiation, asymmetric division, and cell cycle transition (7). To understand the genetic underpinning of this unusual cell cycle, the genomes of *Caulobacte*r strains have been well studied over the years, yet not much has been reported on *Caulobacter*

plasmids (8,9). Plasmids are extra-chromosomal, independently replicating, linear or circular DNA strands (10). They are present in many bacterial strains and been modified through biotechnology techniques to be used for the addition, modification, or knock-out of genes (11,12). The plasmids of Alphaproteobacteria have been found to fall into 3 groups based on size (14) with an average size of 4,623 bp, 68,377 bp, and 483,939 bp, respectively. The larger plasmids within the Alphaproteobacteria are further classified as *repABC*-type plasmids based on their replication genes (14). These plasmids also have similar *parAB* genes, which are involved in the partitioning of the plasmids during cell division (15).

Caulobacters reside in soil, freshwater, and saltwater environments (4), but have been found to be more abundant in soil than in aquatic environments (16). Whitman et al. (2), while looking at interactions between soil minerals and bacteria, found *Caulobacter henricii* to be significantly enriched in their ferrihydrite mineral sample. Ferrihydrite is the main iron oxide precursor in soil, and fixes heavy metal cations, such as Cd^{2+}, Cu^{2+}, and Zn^{2+} (17). This interaction of ferrihydrite with heavy metals has been utilized by soil scientists involved soil conservation.

As indicated above, recent studies have shown many Caulobacters to be plant growth promoting bacteria (18,19). Plant growth promoting bacteria or PGPB have been found to both promote growth and protect the plant from stress and disease. Luo et al. (18) found that *Caulobacter* RHG1 increased leaf number and size, as well as lateral root formation in *Arabidopsis* plants. Similarly, Yang et al. (3) detailed the potential

biotechnological application of *Caulobacter* strain RHGG3 in relation to both its plant growth promoting and heavy metal resistance.

To learn more about how Caulobacters interact with their environment, I identified the plasmid sequences associated with *Caulobacter* genomes in GenBank, an online database for sequences. The plasmids were then grouped and further analyzed to look for important functionality that they could bring to the host *Caulobacter* strain. For example, I found that the plasmid in the CB4 strain conferred heavy metal resistance to the CB4 strain. The results of these analyses are presented in Chapter2.

Many of the *Caulobacter* strains have been shown to be difficult to electroporate (20). This is mainly attributed to the S-layer, an array of ring structures each comprised of six subunits of the RsaA protein and stabilized with Ca^{2+} (21). For example, a mutant S-layer deficient *C. crescentus* CB2 was shown to have 10 times the number of electroporation transformants in relation to the wild type CB2 strain (20). Similarly, the wild type *C. henricii* CB4 proved difficult to electroporate in an experiment with a pBR322 plasmid containing two 250 bp sequences matching the CB4 plasmid *copA* gene. To determine whether the problem lay with the CB4 strain or the plasmid, the experiment was replicated with pXylTn5, a plasmid containing a transposon that is known to randomly integrate into *Caulobacter* genomes in the presence of xylose (22). Again, no transformants were obtained even though a control experiment with CB15, a close relative of CB4 yielded approximately 100 transformants/plate. Therefore, we hypothesized that the CB4 S-layer might be interfering with the electroporation process.

Alternatively, the inability of CB4 to take up foreign DNA could also be attributed to its EPS, or exopolysaccharide layer. In *C. crescentus* the EPS is a tetrasaccharide capsule that is not easily removed through washing (23). We have observed that CB4 cells readily form clumps and electron microscopy images of CB4 have shown that an EPS layer was present on the surface of CB4. Chapter 3 describes as series of experiments performed in an attempt to find conditions that would generate a successful electroporation event.

SARS-CoV 2 and blood clots

The coronavirus SARS-CoV2 has greatly affected the world since its immergence in late 2019. The virus has seen various countries go in and out of lockdown in an attempt to prevent its spread. The University of South Carolina had to end in-person classes in the Spring of 2020 to lessen the spread. During this time, I read every journal article I could find on SARS1, SARS2, and MERS. Originally, the severe cases of the virus were attributed to pneumonia and sepsis, but surprisingly the first large autopsy studies discovered blood clots in most organs and megakaryocyte cells in the lungs, kidneys, and heart (24-26).

The cause of the megakaryocytes and blood clots was and is not fully understood. Based upon the knowledge I had gained from all the SARS articles; I began to devise a hypothesis as to why the blood clots were forming and find existing treatment plans that target these mechanisms. Chapter 4 of my dissertation is a review article hypothesizing the molecular mechanism leading to blood clots in sever COVID-19 patients.

CHAPTER 2

PLASMIDS BRING NOVEL FUNCTION TO *CAULOBACTER* GENOMES

Carter, T. To be submitted to *Current Microbiolog*

Introduction

Bacterial plasmids are extrachromosomal elements comprised of double-stranded DNA. Most well-studied bacterial plasmids confer antibiotic resistance, and some are used for cloning and various gene expression studies. In contrast, naturally occurring plasmids can house genes that are also found in chromosomal DNA as well as genes that have never been found in a bacterial genome [10]. Plasmids often code for proteins that can increase the growth of the host bacterium in the presence of a selection factor, and in the absence of the selection factor, they usually reduce bacterial fitness [2].

Numerous plasmids have been identified in the phylum Proteobacteria due to the symbiotic relationships that these bacteria have with plants and animals [3]. In the case of Alphaproteobacteria, the majority of known plasmids have been found in *Rhizobiales* (143 plasmids), *Rhodospirillales* (122 plasmids), *Rhodobacteriales* (94 plasmids), and *Sphingomonadales* (65 plasmids) [4]. These plasmids have been sorted into two groups based on the similarity of the predicted amino acid sequences of their ParAB and RepABC proteins, which are required for the proper partitioning and replication of the plasmid, respectively [5, 6]. Thus, all of the plasmids found to date in Alphaproteobacteria appear to have diversified from two ancestral types of plasmids.

One of the best studied Alphaproteobacteria is *Caulobacter crescentus* a gram-negative bacterium with a dimorphic lifestyle. Each cell division results in the production of both a stalked cell and a motile swarmer cell that has a single flagellum and multiple pili [7]. After a period of growth, the swarmer cell loses the flagellum and pili and then

synthesizes a stalk to become a mature stalked cell. DNA replication and cell division occur only in the stalked phase of the life cycle [8]. Since *C. crescentus* has a well-known and easy to study cell cycle, it has been developed as a model organism for studying cellular differentiation, asymmetric division, and cell cycle transition [9, 10]. For example, the transcriptome analysis of the cell cycle [9], the genome nucleotide sequence [11], and the essential genome [12] of *Caulobacter crescentus* have been studied extensively.

While much is known about *Caulobacter* genomes [13, 14], not much is known about *Caulobacter* plasmids [15]. Most of the sequenced *Caulobacter* genomes uploaded to the online database GenBank do not contain plasmids. However, a few *Caulobacter* plasmids have been identified including those present in the CB4, K31, FWC26 and FWC2 wild type strains. The Local Adaptation Hypothesis [16] lays the groundwork for why only some *Caulobacter* strains would have plasmids since Caulobacters inhabit a wide variety of environments, and a plasmid could provide genes needed for survival in a particular environment. However, when the bacteria do not live in the presence of an environmental stressor such as a heavy metal, a plasmid containing genes coding for proteins that confer heavy metal resistance would not have the ability to increase host fitness, and therefore the bacteria could benefit from not having to maintain the plasmid. This study analyzes the previously identified plasmids as well as several previously unrecognized *Caulobacter* plasmids and shows that both types of Alphaproteobacterial plasmids can be found among *Caulobacter* strains. In addition,

we demonstrate that the *C. henricii* CB4 plasmid provides enhanced heavy metal resistance to the host cells.

Methods

Bioinformatic analyses

The *repC* nucleotide sequence from K31p1 (accession NC_010335) and the *repB* nucleotide sequence from the CB4 plasmid (accession CP013003) were submitted to BLASTn in the GenBank database [17] to identify homologous sequences in other *Caulobacter* genomes. The *Caulobacter* sequence matches above 40% predicted amino acid identity for the *repB* or *repC* nucleotide sequence were further investigated for the presence of the *mob* and *par* genes. Since plasmids should have circular genomes, the nucleotide sequences of the presumed plasmids were downloaded from GenBank and analyzed with UGENE [18] for sequence overlap within the ends of the contigs. In contrast, a contig representing a portion of a chromosomal sequence would be part a linear stretch of DNA and would not be expected to have overlapping ends. All plasmid sequences examined except that of the ROOT1455 plasmid had overlapping sequences at the ends of the contig. In contrast, the ROOT1455 contig appears to be missing some of the plasmid sequence. The remaining plasmids were then trimmed to unit length and uploaded to the RASTtk [19] annotation servers for gene annotation. The annotated nucleotide sequences were then input into the Mauve software [20] for alignment with the nucleotide sequences of the other plasmids in the same group. In addition, the K31p1, K31p2, and CB4 plasmid sequences were analyzed using the PATRIC Protein

Family Sorter to predict the contributions of the plasmid encoded proteins to the functional pathways of the host cells. Also, since several genes on the CB4 plasmid were predicted to code for proteins that would contribute to heavy metal resistance, the amino acid sequence of each gene on the CB4 plasmid was then used as input into BLAST to identify additional heavy metal resistance genes. Genes were considered homologous if they had at least 40% predicted amino acid identity with at least 60% query coverage and an e-value $<10^{-5}$. To determine whether some genes might be co-expressed from the same promoter, regions containing heavy metal resistance genes were examined and contiguous genes separated by fewer than 40 bp were considered to be expressed as an operon since it is unlikely that there would be sufficient space for a separate promoter. This approach is deliberately conservative, and there may be fewer operons than we proposed. Thus, our transcript analysis might include some redundancy.

Copper resistance

To measure resistance to copper, a 200 ul aliquot of an overnight culture of CB4 or NA1000 was added to 5 mL of PYE [21] along with varying amounts of 10 mM $CuSO_4$. After incubation for 24 hours at 30°C, growth yield was measured at 650 nm with a Klett-Summerson colorimeter. For the mid-log phase growth assay, a 200 ul aliquot of an overnight culture of CB4 or NA1000 was added to 10 mL of PYE and allowed to grow at 30°C. When the cultures had grown to half of the expected level, 8 ul of 10 mM $CuSO_4$ was added to each culture tube, and growth was monitored for 4 hours to determine the impact of the $CuSO_4$ on the growth rate.

Quantitative PCR

For the initial experiment, an overnight culture of CB4 was divided into four tubes containing PYE and 16 uM $CuSO_4$, 8 uM $AgNO_3$, 100 uM $ZnCl_2$, or no addition. Precursor experiments showed that these metal concentrations did not inhibit CB4 growth. After 30 minutes at 30°C, total RNA was extracted from each tube using the PROMEGA Bacterial RNA kit. DNaseI (Invitrogen) was used to eliminate any remaining dsDNA, and PCR experiments confirmed that no dsDNA was present. Subsequently, a ProtoScript II First Strand cDNA Synthesis Kit was used to create a cDNA library. The resulting cDNA was used in a PCR reaction with each of the primer combinations (Supplementary Table B.1), and an aliquot of the products was subjected to agarose electrophoresis to estimate the amount of cDNA present from each gene of interest. qPCR data was obtained from a BIOSYSTEMS 7300 utilizing the Luna Universal qPCR Master Mix (New England Biolabs). Each sample and each gene were analyzed in duplicate, with *rho* as the reference gene. The sample with no added metals was used as a control. Subsequently, expression of operon 2 was measured by qPCR with CB4 cultures grown with three differing concentrations of copper, with 2 runs for each sample. Similarly, expression of operons 4 and 5 were analyzed after growth with 16 um copper for 30 minutes, with 3 runs for each sample, and the expression of operons 1, 3, 4, 5, 6, 7, 8, and 9 was determined after growth with 16 um copper for 30 minutes, with 2 runs for each sample. All genes determined to be induced by copper, displayed a similar increase in expression across all experiments. However, the relative increase in

expression for operon 4 was much more variable due to its extremely low expression in the absence of copper.

Results

Caulobacter plasmids

As indicated above, Proteobacterial plasmids have previously been grouped based on their partitioning (*parAB*) and replication (*repABC*) genes [4]. Consequently, the *repC* nucleotide sequence from K31p1 and *repB* nucleotide sequence from CB4 were used to identify homologous genes in *Caulobacter* genomes present in the GenBank database. Some of the matching sequences were from sequences previously designated as *Caulobacter* plasmids, and others matched individual contigs in partially sequenced *Caulobacter* genomes that were present in the database. Unfortunately, most bacterial genomes present in GenBank are a collection of contigs that represent a fragmented genome since many laboratories have not switched to PacBio sequencing technologies [22]. However, when plasmid *repC* or *repB* genes were found on a contig, our analyses indicated that the contig represented the complete sequence of a plasmid that is associated with that particular *Caulobacter* strain (except for the Root1455 plasmid as noted in Methods). The plasmids identified by this analysis also contained the *parAB* genes which would be required for the partitioning of the plasmid during replication. The nine plasmids identified from seven *Caulobacter* strains ranged in length from 45,171 bp to 420,617 bp (Table 2.1).

Table 2.1. Features of the nine plasmids from seven *Caulobacter* strains.

Caulobacter Strain	AP07	CB4	FWC2	FWC26	Ji-3-8	K31	Root1455
Genome Size (mb)	5.62	3.86	5.25	4.53	5.26	5.48	5.08
Plasmids	1	1	1	2	1	2	1
Plasmid Size (bp)	285,650	93,084	248,587	1) 298,222 2) 45,171	420,617	1) 233,649 2) 177,878	≥64,657
Number of annotated gene features	268	91	242	1) 279 2) 54	358	1) 213 2 172	≥54

Shintani et al. [4] found that in other Alphaproteobacteria, the average plasmid length was 218 kb, and the size distribution of the plasmids was trimodal with the size of the three groups of plasmids averaging 5 kb, 69 kb, and 484 kb, respectively. Our data are consistent with these groupings except that we did not find any plasmids in the small size range. Initial alignments of all the plasmids resulted in two groups based on the *parAB* and *repABC* amino acid identities (Fig. 2.1, Supplementary Table C.2 & C.3). These two groups of plasmids based on the amino acid identities also corresponded to two different genome size classes. The large-sized group contained plasmids that ranged in size from 177878 to 420617 bp and included the K31p1, K31p2, AP07, FWC2, FWC26p1, Ji-3-8 plasmids (Table 2.2). In contrast, the medium-sized group contained plasmids that ranged in size from 45171 to 93084 bp and included the CB4, Root1455, FWC26p2 plasmids (Table 2.2).

Table 2.2. Nucleotide length of the plasmids from various *Caulobacter* isolates.

Category	Accession (contig number)	Plasmid	Size(bp)
Large	CP049200	Ji-3-8	420,617
	CP033873	FWC26p1	298,222
	AKKF01000(205,167,003)	AP07	285,650*
	PEBF01000002	FWC2	248,587
	NC_010335	K31p1	233,649
	NC_010333	K31p2	177,878
Medium	CP013003	CB4	93,084
	LMFQ01000010	Root1455	>64,657
	CP033874	FWC26p2	45,171

The genes required for maintenance of the plasmid, (the replication, mobility, and partitioning genes) were located together and in the same order in a conserved region of each of the medium-sized plasmids (Fig. 2.1). In contrast, the plasmid maintenance genes were scattered in the large-sized plasmids and gene order was not conserved (Fig. 2.2). Also, the K31p2 plasmid did not possess a *repC* gene. RepC is the replication initiator in other Alphaproteobacteria (23). However, since the K31p1

plasmid does possess a *repC* gene, we hypothesized that the RepC protein produced from this plasmid could initiate the replication of both K31 plasmids.

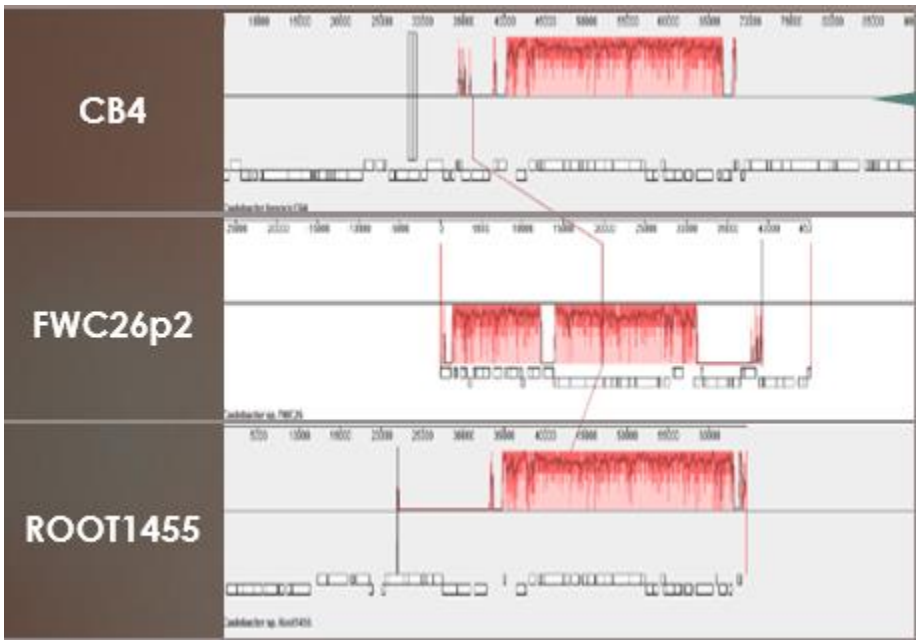

Figure 2.1. Mauve alignment of the medium-sized plasmids.
The red areas represent regions of nucleotide similarity between plasmids which includes replication, mobility, and partitioning genes in the same order in each of the plasmids.

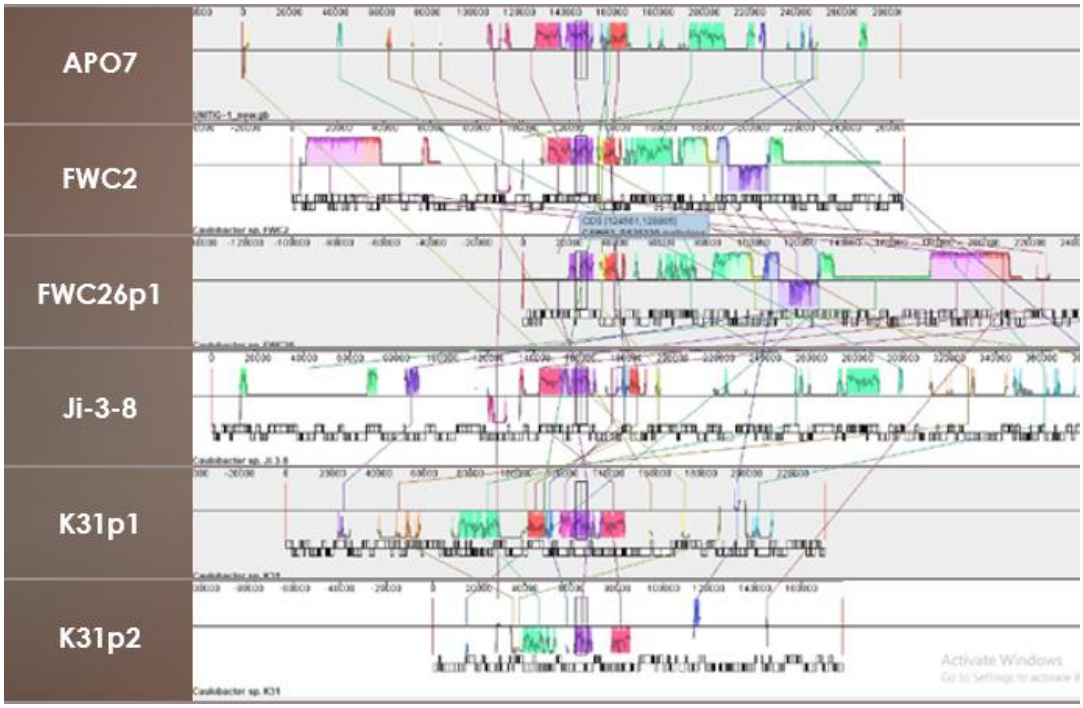

Figure 2.2. Mauve alignment of the large-sized plasmids.Colored areas are areas of homology as determine by Mauve. The pink areas contain the *repC* gene, the purple areas contain *parB* gene, and the teal areas contain *repAB*, *mobA*, and *parA* genes.

Our analyses also provided evidence that a plasmid from the medium-sized group may have integrated into the K31 genome (Fig. 2.2). The *copABCD* genes, RND genes, and *czc* genes have the same gene order in the K31 genome as they do in the CB4 plasmid (Fig. 2.2). However, the *repABC* and *parAB* genes are missing from this region of the K31 chromosome, perhaps due to selection since their presence might interfere with the replication of the K31 genome.

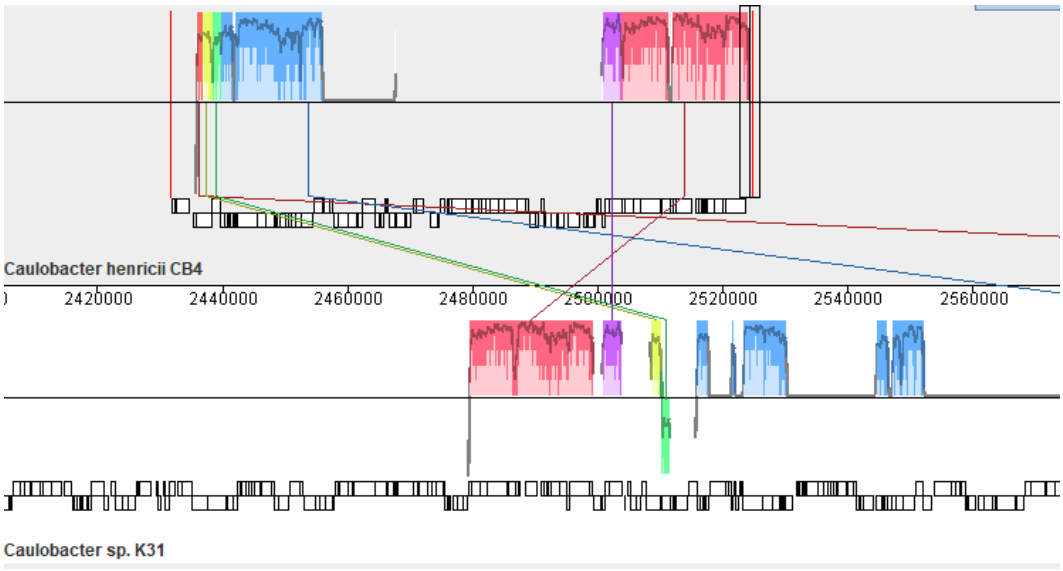

Figure 2.3. Mauve alignment of CB4 plasmid and K31 plasmid. The blue areas contain the RND genes and *CopABCD* on CB4 in the same gene order as those in the K31 genome except that the K31 genome includes a space between the two CB4 plasmid operons. The red areas contain the *czc* genes found on the CB4 plasmid in the same gene order as those in the K31 genome.

As indicated above, K31 houses two large plasmids that contain 212 and 172 genes, respectively, and the genome sequences of these two plasmids are present in the PATRIC database [24] along with that of the CB4 plasmid. Therefore, we were able to analyze the functional groupings of the proteins that are predicted from the genes on these plasmids. Many of the K31 plasmid genes code for proteins that do not have homology to any known protein. However, the genes that code for proteins with annotated functions could provide considerable metabolic versatility to the K31 host bacteria (Table 2.3). In contrast, the genes with predicted functions in the smaller CB4 plasmid are all involved in heavy metal resistance. The FWC26p1 plasmid also has *CopABCD* and *CzcABC* operons similar to those depicted in Fig. 2.3. The two sets of

heavy metal resistance genes are also present in the AP07 and FWC2 genomes but are not found on the AP07 or FWC2 plasmids.

Table 2.3. Pathway assignments for proteins encoded in the K31p1, K31p2, and CB4 plasmids.

Pathways	K31p1	K31p2	CB4
Amino Acid Metabolism	+	+	-
Biosynthesis of Polyketides	+	-	-
Biosynthesis of Secondary Metabolites	+	+	-
Carbohydrate Metabolism	+	+	-
Energy Metabolism	+	-	-
Heavy Metal Resistance	-	-	+
Lipid Metabolism	+	+	-
Metabolism of Cofactors and Vitamins	+	+	-
Metabolism of Other Amino Acids	+	+	-
Nucleotide Metabolism	+	-	-
Xenobiotics Degradation and Metabolism	+	+	-

Characterization of heavy metal resistance conferred by the CB4 plasmid

The C*. henricii* CB4 plasmid contains nine operons that include 21 heavy metal resistance genes (Fig. 4). The *Cue* and *Cus* operons (2 and 9) have previously been

shown to be involved in copper efflux and sensing [25,26]. In contrast, *Cop* operon 5 is predicted to mediate the homeostasis of copper, with the ability to both import and export copper ions [27]. The efflux RND, or resistance nodulation division, transporter genes (Operon 4) code for proteins that form an efflux pump spanning the inner and outer membrane of bacterium [28]. Copper-translocating P-type ATPases (Operon 1) are transmembrane proteins with a cation-binding site for catalytic activation and cation translocation [29]. In addition, the CB4 plasmid contains *czc* genes (Operons 6, 7, and 8) that code for proteins involved in resistance to cadmium, zinc, and cobalt.

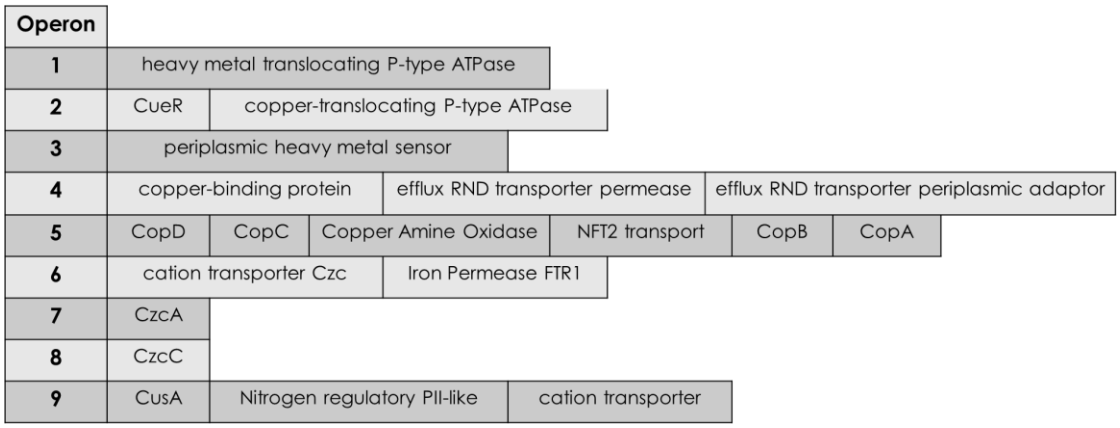

Figure 2.4. Heavy metal resistance gene operons of the CB4 plasmid.

Copper Resistance

Copper in low concentrations poses no threat to bacteria and actually is required for growth since some enzymes are only active when they contain a bound copper ion. However, copper is cytotoxic in higher concentrations [30]. To determine the effect of the CB4 copper resistance genes, growth of CB4 and *C. crescentus* NA1000 was compared in the presence of copper. NA1000 is a well-studied *Caulobacter* strain that

has seven copper resistance genes in its genome. In contrast, the CB4 genome contains a single annotated copper resistance gene, but as indicated above, there are 21 additional copper resistance genes in the CB4 plasmid. Consistent with the presence of extra copper resistance genes, CB4 was able to grow in 16 uM $CuSO_4$ while NA1000 did not grow at this concentration of copper (Table 2.4). The increased copper resistance observed with CB4 was hypothesized to result from the induction of some or all the copper resistance genes present in the plasmid.

Table 2.4. Growth assay of CB4 and NA1000 in the presence of copper.

Strain	**CuSO4 added**	**Final OD**
NA1000	none	0.9
	16 uM	0.02
CB4	none	0.92
	16 uM	0.87

To further analyze the effects of copper on the growth of CB4, copper was then added to cultures of both CB4 and NA1000 at mid-log phase. The 16 um $CuSO_4$ did not slow the growth rate of CB4, while the NA1000 growth rate slowed to 34% of the growth rate of the control sample (Fig. 2.4, Supplementary Table B.4).

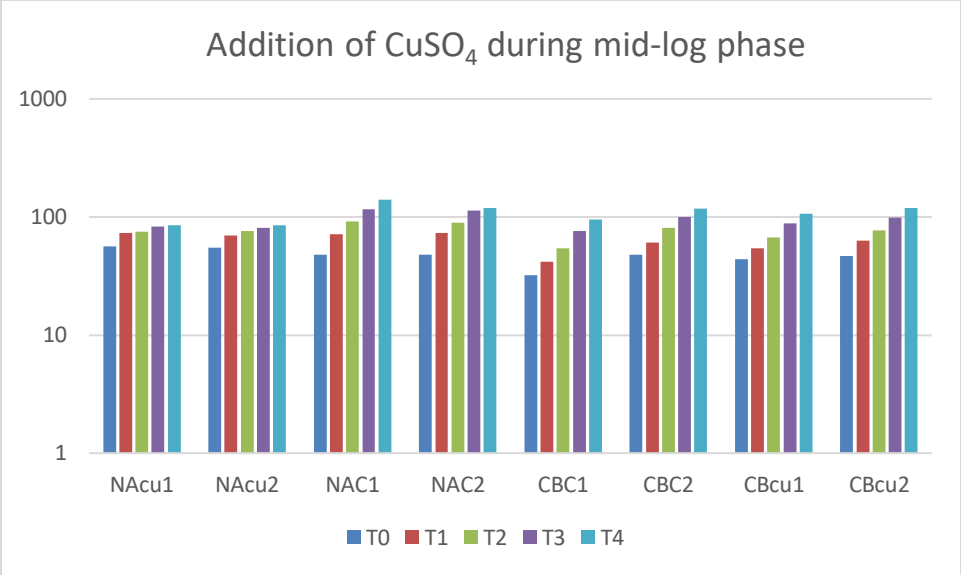

Figure 2.5. Logarithmic growth analysis of CB4 and NA1000 when $CuSO_4$ was added during mid-log phase. T0 is Klett-Summerson reading at the time the $CuSO_4$ was added to the experimental tubes. T1, T2, T3, T4 are number of hours from addition of $CuSO_4$.

To measure the effect of the presence of heavy metals on the expression of the heavy metal resistance operons, RT-PCR was performed for one gene in each of the nine presumed heavy metal resistance operons on the plasmid. The operon with the largest relative change in expression after the addition of copper or silver was the second operon which codes for the Cu(I)- responsive transcription regulator (CueR) and the copper-translocating P-type ATPase (Cop*A*) (Table 2.5). CueR with bound copper binds to the *copA* promoter and induces expression in *E. coli* [31]. Similar results with increased CueR expression were found in *E. coli* 30 minutes after copper induction (32). Therefore, we propose that CueR performs a similar function in *C. crescentus*. In addition, the expression of all the operons except Operon 8 was increased in the presence of copper. Similarly, the expression of all of the operons except 4 and 8 were

induced by silver, and the expression of all operons except Operon 4 was induced by zinc. Cross induction of copper resistance genes has been previously shown with both zinc and silver (33,34).

Table 2.5. Relative expression after the addition of 8 uM of $AgNO_3$, 16 uM of $CuSO_4$, or 100 uM of $ZnCl_2$.

$2^{-\blacktriangle\blacktriangle CT}$	Operon	1	2	3	4	5	6	7	8	9
Sample	Ag	2.1	21.4	10	0.3	8.3	14	2	0.4	1.2
	Cu	3.9	64.6	12.7	1.2	20	12.7	4.7	0.5	2.7
	Zn	2.1	2.4	2.9	0.7	1.8	46.7	6.8	2.7	2.2

Discussion

Our laboratory's previous analysis of 12 *Caulobacter* strains identified three plasmids based on agarose gel electrophoresis [15]. In contrast, the current study was more comprehensive since it was based on a nucleotide sequence analysis of more than 70 *Caulobacter* genomes available in GenBank prior to October 2020. As a result, we were able to verify the presence of the CB4 plasmid and identify eight additional plasmids in six different *Caulobacter* strains. Previous studies [5, 6] had defined three plasmid groups based on size in the Alphaproteobacteria class: large (~483,939), medium (~68,377), and small (~4,623). All the *Caulobacter* plasmids identified in this study fall in either the medium or large sized groups. No small *Caulobacter* plasmid has been identified to date, but our search criteria would not have identified small plasmids

that might be present in incompletely sequenced *Caulobacter* genomes. The *Caulobacter* plasmids in the large-sized group ranged from 177,878 bp to 420,617 bp. The medium-sized group ranged from 45,171 bp to 93,084 bp. All the plasmids contained the required plasmid maintenance genes (*repABC* and *parAB*), except for K31p2 which did not have an annotated *repC* gene. The RepC protein has been found to function as the replication initiator protein, and the K31p1 RepC protein could be further investigated to see if it is functioning as the replication initiator to substitute for the missing *repC* gene in K31p2.

A PATRIC protein pathways analysis showed that the K31p1 and K31p2 plasmids code for proteins that could be involved in a multitude of metabolic pathways, suggesting that these plasmids provide K31 with the ability to degrade a much wider variety of environmental compounds. In contrast, aside from the plasmid maintenance genes, all of the genes with identified functions in the CB4 plasmid are involved in heavy metal resistance, suggesting that the two types of plasmids appear to serve completely different functions. However, both plasmids also contain many hypothetical genes which could have additional valuable functions. The other *Caulobacter* plasmids were also found to have some genes of potential importance. For example, the AP07 and Ji-3-8 plasmids were found to have annotated iron sulfur genes which have been found to serve as biological sensor-switches in Alphaproteobacteria (35), and the Root 1455 plasmid contains multiple chemotaxis genes that could help this strain locate food sources.

All but two of the CB4 heavy metal operons were induced by each of the three metals tested. This result is consistent with our observation that the CB4 plasmid confers a high level of copper resistance to its host strain. Operon 2 which includes genes coding for CueR and a copper translocating P-type ATPase, displayed the largest relative change in expression induced by copper. Similarly, the *E. coli cueR* operon has previously been shown to be induced by both copper and silver and plays an important role in copper resistance [36,37]. In addition, Operons 6 and 7 were induced by copper even though they code for cadmium, zinc, and cobalt resistance genes. This result is consistent with previous studies that showed that copper can induce some, but not all, *czc* genes [32].

Since CB4 has both an exopolysaccharide layer, (EPS) (Carter, T and Ely, B, submitted for publication), and the ability to colonize ferrihydrite (38), we propose that it could be utilized to clean up wastewater containing heavy metals. The EPS of bacterial cells has been utilized for bioremediation in heavy metal spills since it binds heavy metals (39-41), and it causes CB4 cells to clump together and precipitate out of solution. Furthermore, a strain similar to CB4 was found to colonize ferrihydrite (38), an iron hydroxide used in the removal of heavy metal ions in wastewater (42). Thus, CB4 with its EPS, heavy metal resistance genes, and ability to colonize ferrihydrite may facilitate heavy metal wastewater cleanup.

CHAPTER 3

ELECTROPORATION INEFFICIENCY IN CAULOBACTER HENRICII CB4

Carter, T. Submitted to *All Results Journal:Biol*, 01/20/2021

Introduction

Caulobacter crescentus is a gram-negative Alphaproteobacterium that divides asymmetrically, resulting in a stalked cell and a motile swarmer cell (1). In addition, it has a well-developed system of genetics (2) that makes it an excellent model system for the study of cellular differentiation, asymmetric division, and cell cycle transition (3,4). Unlike the *C. crescentus* strains, the wild type strain *C. henricii* CB4 has received little attention even though it houses a 93 kb plasmid, which contains 21 heavy metal resistance genes (5,7, Carter and Ely submitted). CB4 was isolated from pond water in 1959 displaying a vibrioid morphology and forming bright yellow colonies (6). The nucleotide sequence of the CB4 genome and its plasmid has been determined (7), and an analysis of the results indicated that the plasmid contains genes involved in conjugation so it may be able to transfer itself to other strains of *Caulobacter*.

To facilitate a test for conjugal transfer, we attempted to add a kanamycin resistance gene to the plasmid by transposon mutagenesis. Christen et al. (8) established the essential genome of *Caulobacter crescentus* utilizing transposon mutagenesis from the pXylTn5 plasmid containing a xylose inducible Tn5 transposase. The basic approach was to transfer the plasmid into *C. crescentus* from *E. coli* with selection for the kanamycin resistance conferred by the transposon. This technique proved to be an excellent way to get large numbers of *C. crescentus* mutants (8). We planned to use the pXylTn5 plasmid to transpose the gene for kanamycin resistance into

the CB4 plasmid to provide a marker to select for the transfer of the CB4 plasmid transfer into a *C. crescentus* strain.

A second approach was to modify the pBR322 plasmid so that it contained sequence homology to a copper ATPase gene (*copA*) located on the CB4 plasmid. The resulting pBR322-*copA* plasmid contained the beginning and ending sequences of the *copA* gene flanking a tetracycline antibiotic gene. Since this plasmid is not stable in Caulobacters, once it was transferred to CB4, a homologous recombination event would be needed to disrupt the plasmid copper-translocating P-type ATPase gene and confer tetracycline resistance to the host cell.

Preliminary experiments employing standard electroporation or conjugation techniques did not produce any antibiotic resistant CB4 colonies even though control experiments with *C. crescentus* CB15 were successful. Although conjugation experiments generally work well, Caulobacters are difficult to electroporate due to their paracrystalline protein surface layer, or S-layer (9). Visual and centrifuge assays have shown the CB4 S-layer to be thicker than the CB15 S-layer and could be the reason for the unsuccessful electroporation. Alternatively, CB4 could house an exopolysaccharide layer, or EPS. In CB15 and CB2, the EPS is a tetrasaccharide capsule which could not be easily removed by washing (10).

The S-layer is comprised of a 98 kDa RsaA protein that assembles into six subunit hexagons that combine with other hexagon subunits to create a two-dimensional hexagonal array (11). Ca^{2+} is required for the proper crystallization of the RsaA protein,

and the removal of Ca^{2+} has been shown to disrupt the crystallization (12). S-layers are involved in cellular protection and stabilization (13). In *Caulobacter*, the S-layer is hypothesized to be involved in both ion sensing and allowing *Caulobacter* to live in calcium deficient environments (14). S-layer deficient CB2 and CB15 *Caulobacter* strains were found to have a 10 times higher electroporation efficiency compared to their S-layer containing counterparts (9).

Various techniques to destabilize the S-layer have been described. For example, a $LiCl_2$ wash has been shown to decrease the calcium levels and destabilize the S-layer and increase electroporation efficiency (15). Increasing the resistance utilized during electroporation has been demonstrated to increase electroporation efficiency in S-layer *Caulobacter* strains as well (9). Unrelated to the S-layer, it has been shown that growing the bacterium in glycine can improve electroporation efficiency in various bacteria (16, 17). Finally, unmethylated plasmids were shown to incorporate at a higher frequency than methylated plasmids (18). Since our initial attempts to move plasmids into CB4 were not successful, these techniques were used in combination and independently in an attempt to improve electroporation efficiency in CB4 with no success.

Methods

Plasmids

The pXylTn5 plasmid (8) was obtained from Dr. Beat Christen (ETH Zurich). To construct the pBR322-*copA* plasmid (Figure 3.1), primers for the two flanking regions of the *copA* CB4 plasmid gene were designed with restriction sites added on the end of the

primers and used to amplify the beginning and end regions of the *copA* gene with PCR (Supplementary Table C.1). Concurrently, the pBR322 plasmid was cut with *Bsm*I and *Ava*I (Fig. 3.1) and the resulting fragments were separated by agarose gel electrophoresis. The larger section of the cleaved pBR322 plasmid was extracted, purified, and ligated to the *copA* BsmF2 and AvaR2 PCR fragment. The ligated plasmid was transformed into *E. coli* S17 (19) and then plated on LB (20) tetracycline (1 ug/ml) plates. A tetracycline resistant colony was purified, grown overnight in LB, and the pBR322 plasmid containing the distal part of the *copA* gene was isolated. The plasmid was digested with *Bsm*I and *Ava*I to confirm the presence of the *copA* gene fragment. The newly constructed plasmid was then digested with *Eco*R1 and *Cla*I, purified as above, and ligated with the *copA* EcoF1 and ClaR1 PCR fragment. After the ligated construct was transformed into *E. coli*, purified and re-isolated, the proper configuration of the pBR322-*copA* plasmid was confirmed by PCR using the EcoF1 and AvaR2 primers. The pBR322-*cop*A plasmid also was transformed into a DCM^-/DAM^- *E.coli* strain (ZYMO mix n go), and both the methylated and unmethylated forms of pBR322-*cop*A were used for the remainder of the experiments.

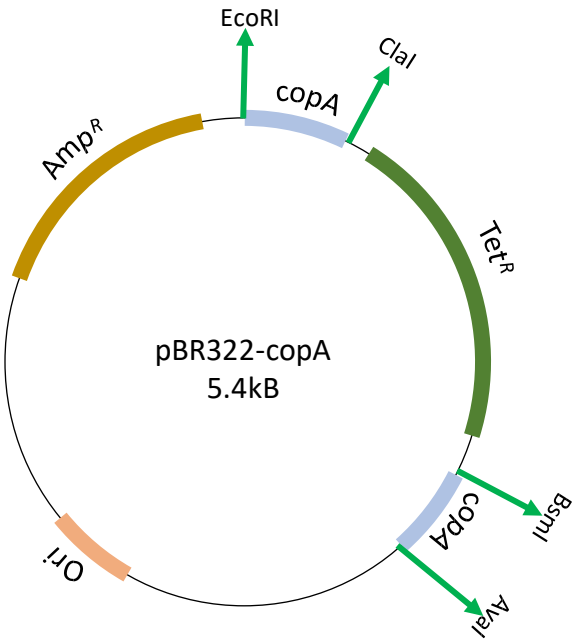

Figure 3.1. Structure of pBR322-copA plasmid. Two ~250 bp segments from the CB4 plasmid *copA* gene were ligated in at *Eco*RI/*Cla*I and *Bsm*I/*Ava*I cut sites.

Electroporation

To prepare electrocompetent cells, CB4 and NA1000 were grown in 100 mL PYE (21) to mid-log phase. The samples were divided into 50 mL centrifuge tubes and spun at 7000 x g for 5 minutes, and the resulting cell pellets were resuspended in 20 mL of sterile deionized water. The samples were then spun and resuspended as before. The final pellets were resuspended in 2 mL of 10% glycerol, spun at 4000 x g for 5 minutes, and resuspended in 400 ul of 10% glycerol. Finally, 200 ul aliquots were prepared with half used right away and half stored in the -70°C freezer.

For electroporation, 40 ul of the CB4 electrocompetent cells were placed in a 0.5 mL tube in, and 2 ul plasmid DNA was added. Subsequently, 40 ul of the CB4/plasmid mixture was placed in a 0.2cm Bio Rad (Hercules, CA) Gene Pulser cuvette the and subjected to a 2.5-kV shock with the capacitor set at 25 uF (microfarad) and the resistance at 200 ohms in a Bio Rad Gene Pulser electroporator. With a 0.2 cm cuvette gap, a 4.5 to 5 msec time constraint was expected at 200 ohms. After the shock, the contents of the cuvette were mixed with 1 ml PYE, transferred to a sterile test tube, and incubated at 30°C for 2 hours before 200 ul of each sample was plated on PYE plates containing the appropriate antibiotic. When using the pXylTn5 plasmid, the plates also contained 100 ul of a 10% xylose solution to induce transposition.

Conjugation procedure

The *E. coli* BC1490 which houses the pXylTn5 plasmid and CB4 cultures were grown overnight in LB or PYE medium, respectively. To initiate conjugation, one mL of the CB4 culture was gently mixed with 0.1 mL of the *E. coli* BC1490 culture. After the mixture was filtered through a Millipore HA 0.45 uM filter, the filter was then placed on a PYE plate and incubated overnight at room temperature. After the incubation, the filter was placed in sterile test tube with 500 uL PYE, and the bacteria were resuspended by vortexing. Subsequently 200 uL of the bacteria suspension was plated on each of two PYE plates containing the appropriate antibiotic to select for the presence of the plasmid and nalidixic acid (20 ug/mL) to select against the *E. coli* donor strain. Each

mating experiment was performed twice for replication of results. Plates were then incubated at 30°C for 2-3 days until colonies appeared.

Results

The pBR322-*copA* plasmid contains two sections of the copper-translocating P-type ATPase *cop*A gene (approximately 250 bp each) that flank a tetracycline gene and are identical to the corresponding regions of the CB4 plasmid (Fig. 1). Since the pBR322-*copA* plasmid cannot replicate in *Caulobacter*, homologous recombination would be needed for the host bacterium to acquire tetracycline resistance after the introduction of the plasmid. Initially, the standard electroporation procedure was used in an unsuccessful attempt to get the plasmid into CB4. Of note, CB4 tended to aggregate into clumps that were difficult to disperse during the preparation of the electrocompetent cells, in comparison to NA1000 where the bacteria goes back into solution from the pelleted state without much agitation. CB4 gave a time constraint of 3.4-3.6 msec at the standard electroporation settings compared to the 4.6-4.8 msec obtained with other *Caulobacter* strains. Each experiment was run in duplicate and then it was replicated 4 separate times. No CB4 transformants were obtained from any of these experiments.

To further investigate, we attempted to transform the pXylTn5 plasmid into both CB4 and NA1000. The standard protocol was followed and approximately 100 transformants were obtained with NA1000, and no transformants were obtained with CB4. The experiment was replicated with the same results. Since the standard procedures were not working, we decided to alter both the variables involved in the

preparation of the electrocompetent CB4 cells and the electroporation procedure itself as described below.

Varying resistance during electroporation

Gilchrist and Smit (9) demonstrated that increasing the resistance from 200 or 400 to 600 or 800 ohms increased the number of transformants for S-layer containing Caulobacters. Also, Spath et al. (18) showed that the use of an unmethylated plasmid can increase transformation efficiency. Therefore, CB4 electrocompetent cells were prepared according to standard protocol and electroporation experiments were performed at 200, 400, 600, and 800 ohms. For each level of resistance, transformations with both a methylated and an unmethylated plasmid were attempted in duplicate, and the time constraints did increase in relation to the increase in resistance. Although increasing the resistance had previously increased the number of transformants in S-layer containing Caulobacters (9), no transformants were observed for any of the 16 samples. As a control an additional aliquot was plated on antibiotic-free control plate to verify bacterial viability.

$LiCl_2$ Wash

A $LiCl_2$ wash has been shown to disrupt the Ca^{2+} component of the S-layer and increase electroporation efficiency (15). Therefore, a $LiCl_2$ wash was added after the initial pelleting of CB4. The pelleted CB4 cells were resuspended in 5 mL of 5M $LiCl_2$ and held on ice for 30 minutes, pelleted, then resuspended in 5 M $LiCl_2$ and held on ice for an additional 30 minutes. The $LiCl_2$ procedure called for the use of SMEB as the

resuspension and electroporation buffer instead of using the 10% glycerol as called for by the standard procedure. Using the SMEB after the $LiCl_2$ resulted in a 0.1 msec time constraint and a “pop” of the cuvette when a spark was emitted. One cause of this is can be a high salt concentration. To bypass this problem, a 10% glycerol solution was used during the wash and final preparation of the electrocompetent cells. This modified procedure resulted in the expected time constraints at the 200 and 400 ohms resistance. Again, the experiment was performed with both a methylated and unmethylated plasmid at both 200 and 400 ohms, and no transformants were obtained. To confirm cell viability, 400 ul of one of the $LiCl_2$ washed electroporation samples was plated on a PYE with no antibiotics and cell growth occurred at the expected rate.

Glycine Growth Media

In other bacteria, adding glycine to the growth medium has been shown to increase electroporation efficiency (16,17). CB4 was unable to grow in the previously established 1% glycine concentration which had been shown to increase electroporation efficiency. The highest concentration of glycine that allowed CB4 to grow was 0.1%, and electrocompetent cells were prepared from CB4 cells grown in the presence of 0.1% glycine. For electroporation, both the methylated and unmethylated pBR322-cop plasmids were used at 200 and 400 ohms resistance. The experiment was performed in duplicate and the expected time constraints were obtained, yet none of the runs resulted in any transformants.

EPS

Caulobacter can possess an exopolysaccharide, or EPS layer than acts as another physical barrier to the cell (10). Electron microscopy showed that an EPS layer was present on CB4 cells, as did the clumping of cells during the cell preparation procedure (Fig. 3.2). Growing bacteria in the presence of 0.7 mM EDTA has been shown to disrupt the EPS and increase electroporation efficiency in other gram-negative bacteria (22), but CB4 did not grow at that concentration of EDTA. *Caulobacter* requires 0.5 mM Ca++ for optimal growth (23) and is sensitive to calcium levels when the S-layer is disrupted (14). CB4 was able to grow at 0.3 mM and 0.4 mM, but not 0.7 mM, EDTA. Therefore, 30 mL cultured of CB4 with 0.3 mM or 0.4 mM EDTA were grown to 30 Kletts, spun down, and washed with 10% glycerol four times. The cells were then pelleted and resuspended in 160 ul of 10% glycerol. Subsequently, 40 ul of the electrocompetent cells were mixed with 1 ul of methylated or unmethylated pBR322-copA and electroporated with the standard procedure. All runs resulted in zero transformants. A control experiment with electrocompetent cells created from CB4 grown in both PYE and PYE with 0.4 mM EDTA resulted in 1.25×10^5 CFU/mL of the PYE-grown CB4 competent cells, and no colonies were observed when 20 ul of the EDTA-grown CB4 competent cells were spread on PYE plates. Therefore, we concluded that growth in EDTA lowered the survival rate during the preparation of electrocompetent cells to the point that no surviving cells were present.

(a)

(b)

Figure 3.2. Electron microscope images of *C. henricii* CB4. (a) The EPS layer surrounding the CB4 bacterium is visible as a halo. (b) A clump of CB4 cells.

Table 3.1. Description of altered variables to increase electroporation efficiency.

	Description	Source
Increased Resistance	Increasing the resistance to 600 or 800 ohms has been shown to increase electroporation efficiency in Caulobacters with S-layers.	**[9]**
Unmethylated Plasmids	Unmethylated plasmids (DCM^-/DAM^-) have been shown to increase electroporation efficiency.	**[18]**
$LiCl_2$ Wash	$LiCl_2$ wash used to disrupt Ca^{2+} and RsaA interaction and destabilize the S-Layer	**[15]**
Glycine Growth Media	Glycine added to growth media has been shown to increase electroporation efficiency.	**[16,17]**
EPS Disruption	Bacteria grown in the presence of EDTA has been shown to disrupt the exopolysaccharide layer.	**[22]**

Conjugation experiments

Conjugation can also be used to transfer a plasmid from *E. coli* to *Caulobacter* (24). Therefore, conjugation experiments were carried out using the same NA1000 and CB4 bacteria strains with *E. coli* BC1490 which houses the pXylTn5 plasmid. Approximately 400 colonies were obtained with NA1000 as a recipient and no colonies were obtained with CB4 as a recipient. This experiment was repeated with *C. crescentus* strain SC1004 and CB4 with similar results (Fig. 3.3). Alternatively, conjugation experiments were carried out with CB4 and *E. coli* HB101 which houses the pRK290 plasmid. The pRK290 plasmid houses a RK2 replicon which has been shown to be stable in *Caulobacter* (25), but again, no colonies were obtained from the conjugation with CB4.

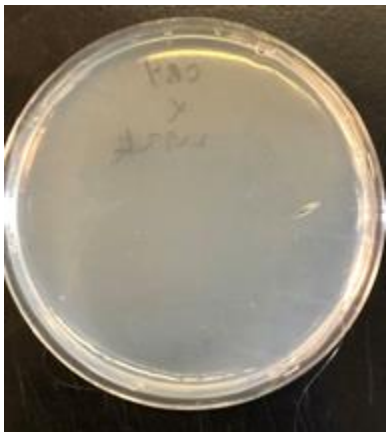 (a)  (b)

Figure 3.3 Conjugation results with CB4 and BC1490 (1a), and *C. crescentus* SC1004 and BC1490 (1b).

Discussion

Electroporation is a useful technique for the introduction of foreign DNA into a bacterium. Previous work has demonstrated that getting DNA into *C. crescentus* electroporation is more difficult due to its S-layer (9). The S-layer is a crystalline layer consisting of RsaA protein subunits and Ca^{2+} ions. Gilchrist and Smit (9) demonstrated that increasing the resistance increased electroporation efficiency in S-layer containing *C. crescentus* strains. However, our use of this procedure did not result in any CB4 transformants. Other researchers increased bacterial electroporation efficiency by using unmethylated plasmids (17), or growth in glycine (16, 17). However, neither of these procedures was successful with CB4. Also, a $LiCl_2$ wash during the preparation of electrocompetent cells has been shown to disrupt the S-layer by removing the Ca^{2+} ions (15), but this technique also did not result in any CB4 transformants. In addition, we were unable to transfer plasmids into CB4 using standard conjugation techniques.

It is possible that the CB4 S-layer is thick enough so that these techniques do not disrupt it sufficiently to allow for the uptake of foreign DNA. In addition, CB4 also has an extracellular polysaccharide (EPS) layer that may block DNA uptake as well. It also is possible that CB4 produces an endonuclease that cleaves extracellular DNA during the electroporation procedure. However, the inability to transfer a plasmid via conjugation where exposure to an endonuclease would not occur indicates that the primary issue is some type of external barrier(s) that prevents both conjugation and electroporation from occurring. Further evidence for this barrier is that CB4 tends to form clumps of cells during growth (Fig. 3.2), and CB4 cell pellets are difficult to resuspend after centrifugation. Thus, CB4 cells tend to stick to each other in ways that are not observed with *C. crescentus* cells. The role of calcium in S-layer and EPS disruption was also found to decrease cell viability after electroporation. This creates a difficult situation in which disrupting the EPS and S-layer to allow foreign DNA to enter decreases cell viability.

CHAPTER 4

FROM SARS-COV2 TO BLOOD CLOTS, A FURIN CLEAVED S1 BUILDUP

Carter, T. To be submitted to *Viral Immunology*

Abstract

SARS-CoV2 has greatly affected the entire world for the majority of 2020. Many laboratories have been hard at work on developing treatments and vaccines, yet to date no therapeutic approach has been able to greatly reduce the mortality rate. Many patients, especially the young have exhibited mild symptoms or no symptoms at all. In contrast, we hypothesize that in older patients with fewer ACE2 receptors, the furin-cleaved S1 protein binds to most of the available ACE2 receptors, resulting in a cellular build-up of Angiotensin II. This build-up then leads to a cascade of effects that ultimately results in numerous blood clots. Recently several studies have shown that drugs that target the early stages of this SARS-CoV2 molecular cascade pathway are able to lower the mortality rate currently occurring with this deadly virus.

Mini Review

Introduction (background)

SARS-CoV2 has infected over 12 million Americans by late November 2020 (1), and more than 250,000 Americans infected have died due to COVID-19. Even with vaccines on the horizon, a successful reduction in mortality would have great benefit to society. The molecular mechanisms that SARS-CoV2 utilizes are understood well enough to know which molecular interactions to target with therapeutics. As more information is collected on deceased COVID-19 patients, a commonality of blood clots is starting to surface suggesting that blood clots could be the primary cause of COVID-19 deaths (2-4). Therefore, preventing the blood clots, or the molecular cascade that leads to the blood

clots, could result in a decreased mortality rate. This review will detail how the SARS-CoV2 virus could be inducing blood clotting in patients and suggest that several drugs that have been shown to reduce COVID-19 mortality may be disrupting this cascade.

S1 build up

During the initial infection, the SARS-CoV2 virus, like SARS-CoV1 (5), binds to the ACE2 (Angiotensin converting enzyme 2) receptor, and the viral spike protein is cleaved by TMPRSS2. The S2 portion of the spike protein then allows membrane fusion and viral entry (6). SARS-CoV2 has a higher binding affinity to ACE2 than SARS-CoV1 so it is more efficient at this initial stage of infection (7). Another difference between SARS-CoV1 and SARS-CoV2 is the PPC/furin cleavage site located between the S1 and S2 portions of the spike protein. However, this difference does not seem to enhance viral entry into the cell (7). The majority of human proprotein convertases (PPC), such as PCSK3 (furin), are found in the trans golgi network (8). As a result, the S protein is processed almost entirely into S1 and S2 during biosynthesis (7,9). For example, in SARS-CoV2 infected Vero E6 cells, 45% of the spikes found on a SARS-CoV2 virion were cleaved at the S1/S2 site, and in Calu-3 cells 73% of the spikes were cleaved at the S1/S2 site (60). MERS, another coronavirus that houses a furin cleavage site between S1/S2 was also found to be processed by PPC in MERS-CoV infected cells and MERS- S transfected cells, yet the inhibition of the PPC did not affect MERS infectivity (10). Furthermore, the cleaved S1 protein is likely to be protected from degradation due to the interaction of SARS-CoV2's ORF10 with the cullin-2 (CUL2) RING E3 ligase complex (11) which would protect the

cleaved S1 protein from ubiquitin targeted degradation (12). The accumulated S1 protein would be released into the extracellular environment during cellular lysis and could bind to the ACE2 receptors on the surface of nearby cells. The isolated S1 protein has been shown to bind soluble ACE2 (13,14), and Zhao et al. (15) showed that tagged S1 had significant and consistent association with human ACE2. This S1 binding would lead to a cascade of molecular interactions that would result in blood clots as will be detailed below.

Angiotensin converting enzyme 2 (ACE2)

ACE2's main biological function is the conversion of Angiotensin II (AngII) into Angiotensin-(1-7) (16) as part of the Renin-Angiotensin System, or RAS (17). The RAS is a molecular cascade pathway that is involved in hypertension and other cardiovascular disorders (18). Angiotensin II binds to ATR1 (angiotensin type 1 receptor) and ATR2 (angiotensin type 2 receptor) (19,20). AngII mainly acts by binding to ATR1, while the ACE2 product Ang-(1-7) binds to the Mas receptor (21), which promotes a counter-balancing pathway to AngII/ATR1 (22). The viral bound ACE2, or the hypothesized S1/ACE2 complex would result in higher concentrations of AngII, and lower levels of Ang-(1-7) since ACE2 would not be available to convert AngII into Ang-(1-7). A study by Wu et al. (23) showed that the AngII plasma levels were higher than normal in most COVID-19 patients and in all of the critically ill COVID-19 patients. In addition, univariate analysis showed a positive correlation between plasma AngII concentration and COVID-19 severity across 82 non-hypertensive patients. This altered balance would disrupt RAS

as described above. In addition, based on autopsy results of multiple blood clots, and increased numbers of megakaryocytes, it seems that IL-6, a cytokine whose expression has been shown to be induced by AngII (24), may play a vital role in blood clotting.

AngII and IL-6 by way of ATR1

Since an ATR1 inhibitor blocks AngII induced IL-6 production, Clancy et al. (25) concluded that AngII induces the production of IL-6 through ATR1, and IL-6 is essential for the physiological changes induced by AngII (26). In the kidney, AngII has been shown to induce IL-6 production in both human and rat models (27). Furthermore, IL-6 is a downstream byproduct of AngII binding to ATR1, since a blocked ATR1 receptor resulted in lower concentrations of IL-6 (28). In contrast, Ang-(1-7) has the opposite effect and attenuates IL-6 expression (29). Thus, an altered balance of AngII and Ang-(1-7) could lead to high levels of IL-6, and since IL-6 has been shown to increase the expression of ATR1 a feed forward loop would develop to further increase IL-6 levels (28). Evidence that this feed forward loop occurs has been found in critically ill SARS-CoV2 patients who have up to 10 times normal IL-6 levels (30), and these high levels would play a vital role in the molecular cascade that results in blood clots.

Megakaryocytes

Autopsy results in New York left scientists surprised when they found platelet rich thrombi and an increased number of megakaryocytes in the lungs, heart and kidneys of the deceased (2). Megakaryocytes are highly specialized precursor cells that ultimately result in the release of platelets (31). The majority of megakaryocytes are

found in bone marrow, but it is estimated 20-50% of the mature megakaryocyte population enters the blood and ultimately resides in the lungs (32). Two factors would result in the increased concentrations of megakaryocytes seen in the autopsies: 1) increased stromal cell-derived factor 1 (SDF-1) levels would result from AngII binding to ATR1, and increased SDF-1 levels are involved in megakaryocyte localization and platelet formation (33-36); and 2) increased thrombopoietin (TPO) levels also would occur due to the high levels of IL-6 (37). Thrombopoietin (TPO) is involved in the proliferation, differentiation, and maturation of megakaryocytes (38), and IL-6 has been found to directly increase the mRNA expression levels of TPO in HepG2 cell cultures and also increase TPO plasma levels in human cancer patients (37). Thus, increased SDF-1 and/or increased TPO could lead to increased megakaryocyte migration and maturation, resulting in an increased number of platelet-forming megakaryocytes as seen in the autopsy reports.

TF platelets and blood clots

Tissue factor (TF) is a transmembrane receptor involved in blood coagulation (39), and TF platelets are associated with morbidity in severe COVID patients (40). Neutrophils from COVID-19 patients have high TF expression and produce functionally active TF, through neutrophil extracellular traps (NETs) (41). NETs are composed of chromatin and antimicrobial proteins and have been found to play a role in thrombin generation (42). High NET levels occur in many COVID patients (43), and neutrophils are likely to be present in higher numbers since AngII recruits neutrophils in vivo (44). AngII

also stimulates platelets to express TF in a rat model (45), and it can induce platelet shape change, which is required for platelet aggregation (46). In autopsy patients in Houston, the platelets from Megakaryocytes were found to entrap numerous neutrophils within small vessels (47), which would lead to blood clots. Taken together, these factors could account for the severity of blood clotting in COVID-19 patients.

Higher mortality rate in elderly and males could be attributed to lower Ace2 expression thus leading to more blood clots

It has been hypothesized that an increase in ACE2 receptors would lead to an increased severity in COVID disease, yet the groups with the highest levels of ACE2 receptors: females and the young are least at risk (48). This fits in with the hypothesis that the cleaved S1 protein is blocking the majority of the biologically active ACE2 receptors in severely ill patients. In contrast, individuals with more ACE2 receptors might be able to avoid the cascading effects of the AngII buildup since it would be more difficult to block most of the ACE2 receptors. Although the virus would find easier cell entry if there were more ACE2 receptors, more receptors per cell also could result in individual cells binding multiple viruses and fewer cells being infected. Either way, the severe illness present in some SARS-CoV2 cases could be avoided.

Severity blood markers: IL-6 and Syndecan-1

A new study by Wang et al. (49) analyzing the blood of 12 COVID-19 patients found that IL-6 and Syndecan 1 levels were higher in the severe persistent group compared to the recovering group. Syndecan 1 is part of a family of cell surface heparan

sulfate proteoglycans involved in inflammatory and disease responses (50). The higher levels of both IL-6 and Syndecan 1 can be attributed to the higher AngII levels in the cellular environment. As discussed above, high AngII levels increase IL-6 levels, so higher IL-6 levels would be expected in patients with severe COVID-19. Furthermore, Wang et al. (51), showed that AngII increases mRNA expression of Syndecan 1, increases cell-surface Syndecan 1, and speeds up Syndecan 1 shedding in murine macrophages. Another murine study (52) showed that in Syndecan 1 knockout mice, cardiac dysfunction during AngII induced hypertension was reduced. Thus, high Syndecan 1 levels contribute to hypertension-induced cardiac dysfunction. Although IL-6 and Syndecan 1 can be increased by many pathways, their higher levels in the severe COVID-19 patients would be the expected result of increased AngII levels.

Blocking the AngII-induced cascade

Angiotensin II receptor blockers or ARBs have been shown to greatly reduce D-dimer, a biomarker of blood clots, in elderly COVID-19 patients compared to non ARB-users (53). Losartan would be a prime candidate for treatment of COVID-19-induced clots in elderly patients and multiple studies have demonstrated its safety profile (54,55). In addition, the University of Minnesota is currently housing an ongoing Losartan clinical trial (NCT04312009) for hospitalized COVID-19 patients.

Baricitinib, a JAK inhibitor, was recently found to have a 71% mortality benefit in 83 COVID-19 patients (56). The JAK-STAT pathway has been shown to mediate AngII/ATR1 triggered gene transcription. AngII has been shown to elicit JAK pathways in

a G protein-dependent and -independent fashion (57). Furthermore, a rheumatoid arthritis study demonstrated that Baricitinib has an acceptable safety profile (58).

Soluble ACE2 receptor is another viable treatment option. One study showed a decrease in IL-6 and AngII levels, with an increase in Ang-(1-7) after soluble human recombinant ACE2 (shrACE2) was administered through IV (59). Ang-(1-7) is another potential treatment option, based on its counter-effect to AngII/ATR1. Currently a clinical trial (NCT04332666) is underway to determine its efficacy.

Discussion

Blood clots are a common occurrence in severe COVID patients (2). A recent study looking at the blood work of COVID patients saw a significant increase in IL-6 and Syndecan-1 levels between the recovering and severe patients (49). We hypothesize that the cause of these symptoms and blood markers is from the buildup of Angiotensin II (23) caused by the Furin cleaved S1 protein of the SARS-CoV2 virus binding to the ACE2 receptor (7,9), and blocking the conversion of Angiotensin II to Angiotensin-(1-7). This buildup of AngII disrupts the Renin-Angiotensin System and leads to a molecular cascade that results in TF-platelet blood clots (45,46). In addition, this hypothesis accounts for the higher mortality rate in the elderly population as data has shown they have lower ACE2 levels than young individuals (48). Targeting this molecular cascade and the S1 protein could provide valuable therapeutic approaches that would help severe COVID-19 patients. Current clinical trials and research results have proven this to be true (53,56,59). The ongoing Ang-(1-7) clinical trial (NCT04332666) and Losartan

clinical trial (NCT04312009) should have promising results as well. Although blocking ATR1 or inhibiting JAK provides relief due to the increased AngII/ATR1 binding, there is still the problem of lack of Ang-(1-7). Losartan and Baricitinib will improve clotting conditions, but the hypothetical best combination to overcome lack of ACE2 would be either drug in combination with Ang-(1-7), or soluble ACE2.

CHAPTER 5

CONCLUSION

Many people choose to focus on one particular subject during their time as a PhD student, yet I felt expanding my knowledge base to as many topics as I could learn would best prepare me for my future. I have always tried to expand myself in everything I try, from sports to social groups to academic topics. This perhaps could be a result of living with OCD and PTSD and living day to day with my brain trying to focus and obsess on one topic and attempting to push back and actively expand in all areas. During the times of my many surgeries, I read every journal article I could on a variety of topics. This led to an interest in plants, which resulted in me devising a molecular way to confirm the speciation of two *Shortia* plants (1). In Spring 2020 when SARS-CoV2 forced the in-person closure of the University, I read as many articles on the virus as I could. This, along with my previous virion-host knowledge paid off in my creation of the SARS-CoV2 S1 buildup hypothesis found in chapter 4. My path to this point in my career has not been standard by any means. I do believe though, that without all my setbacks I would not be the scientist I am today.

Role of naturally occurring *Caulobacter* Plasmids

Although the genomes of the *Caulobacter* genus had been well studied (2,3), not much was known about the plasmids that were present in many strains. Bioinformatic

searches helped me identify and classify a total of nine plasmids located in seven *Caulobacter* strains. The plasmids all contained the essential genes needed for plasmid replication, partitioning, and mobility: *repABC*, *parAB*, or *mobAB,* except for one plasmid K31p2 which did not have a repC gene to code for the replication initiator protein. This observation could be investigated further to determine if the K31p1 RepC protein is acting as the replication initiator protein for both the K31p1 and K31p2 plasmids since they are housed in the same bacterium. The nine *Caulobacter* plasmids that we identified were then sorted into two groups, based both on size and the nucleotide sequence of the essential plasmid genes that corresponded to the medium and large plasmid groups identified in a previous Alphaproteobacterial study (4).

A PATRIC protein pathway analysis of the K31p1, K31p2, and CB4 plasmids was used to identify the genes on each of the plasmids that correspond to genes with known functions. This analysis showed that the K31p1 and K31p2 plasmids contain genes that participate in various metabolic pathways such as amino acid, lipid, carbohydrate, and xenobiotic metabolism but neither plasmid contained genes related to heavy metal resistance. In contrast, the CB4 plasmid contains 21 heavy metal resistance genes and no genes known to be involved in metabolic pathways. Because of the presence of these heavy metal resistance genes, the CB4 plasmid was selected for further analyses. Since most of these genes were annotated as copper resistance genes, we tested CB4 for growth in $CuSO_4$ and demonstrated that concentrations up to 16 uM CuSO4 did not disrupt the growth of the CB4 strain even though this concentration of $CuSO_4$ totally inhibited the growth of the standard laboratory strain *C. crescentus* NA1000. In addition,

quantitative PCR results showed that $CuSO_4$ induced the expression of 8 of the 9 heavy metal resistance operons.

The ability of CB4 to live in high copper environments could have an important environmental impact since CB4 has been found to colonize ferrihydrite by attaching to it via its sticky holdfast (5). Ferrihydrite is an iron precursor found in soil and has been used in industrial wastewater clean ups (6). Ferrihydrite binds Cd^{2+}, Cu^{2+}, and $Zn^{2+,}$ which are metals that are pumped out of the cell by the *czc*, *cop*, *cus*, and *cue* systems present on the CB4 plasmid. CB4 also possess an exopolysacchride layer, or EPS. Bacterial EPS have been used to pull heavy metals out of wastewater spills (7,8). Therefore, the addition of both CB4 and ferrihydrite to wastewater could be beneficial for removal of the metal ions. One of the problems with ferrihydrite is the difficulty of getting it out of the wastewater solution after it has bound the heavy metal ions. CB4 bound to ferrihydrite could be added to the wastewater to bind the contaminating metal ions. Since CB4 cells tend to form clumps due to its EPS and sink to the bottom of a container, the CB4/ferrihydrite/metal ion complexes then would gradually settle to the bottom of the container and the purified wastewater could be removed from the top of the container. The combination of CB4's heavy metal resistance, EPS, and ability to colonize ferrihydrite could prove beneficial to future wastewater cleanup practices.

Electroporation Inefficiency in *Caulobacter henricii* CB4

C. henricii CB4 like other S-layer containing *Caulobacter* strains has proven difficult to electroporate. Gilchrist and Smit (9) showed that mutant S-layer deficient *C.*

crescentus CB2 had 10 times the electroporation efficiency in relation to the wildtype CB2. Electroporation done simultaneously with CB4 and its close relative *C. crescentus* CB15 resulted in 100 transformants/plate with CB15, but none with CB4.

Experiments were then designed utilizing electroporation conditions found to be beneficial in increasing electroporation efficiency. For example, increasing the resistance of the electroporator from 200 ohms to 400, 600, or 800 ohms has previously been shown to increase electroporation efficiency in S-layer containing *Caulobacter strains* (9). With CB4, the increased resistance settings did not result in any transformants. Similarly, a $LiCl_2$ wash disrupts the Ca^{2+} ions which stabilize the S-layer and has been shown to increase electroporation efficiency (10). Again, the $LiCl_2$ wash with CB4 did not result in any transformants. The addition of glycine to the growth media of bacteria has been shown to increase electroporation but did not result in any transformants with CB4 (11,12).

Since targeting the S-layer did not yield transformants and electron microscopy images of CB4 showed the presence of an exopolysaccharide (EPS) layer which can create a physical barrier around the bacterium (13), we changed our focus to the EPS layer. EDTA has been shown to disrupt the EPS in bacteria and increase electroporation efficiency (14). The addition of EDTA in various concentrations did not result in any electroporation transformants in CB4. Disrupting the S-layer, or EPS through chelators is difficult as Caulobacter is sensitive to low calcium levels when its S-layer is disrupted (15). This sensitivity creates a situation where the cell viability is decreased to low levels

when the S-layer or EPS are disrupted, and calcium levels are low. This dynamic potentially counters any benefit in electroporation efficiency brought on by the S-layer or EPS disruption.

SARS-CoV 2 and blood clots

Autopsies have been conducted to determine what factors lead to the death of COVID patients. The most surprising finding of the first autopsy studies was the presence blood clots in major organs, and an increase in the number of megakaryocytes present in the lungs, heart, and kidneys of the deceased patients (16-18). After reviewing as much of the published data as I could find, I proposed that the furin-cleaved S1 fragment of the spike protein could bind to most of the available ACE2 in the cellular environment. Since ACE2 is required to convert Angiotensin II (AngII) to ANG1-7, blocking ACE2 could lead to a buildup of Angiotensin II (AngII). Angiotensin II is part of RAS, or Renin Angiotensin System (19). Its main target is the ATR1 receptor, and its downstream effects detailed in Chapter 4 would contribute to the molecular cascade that causes the TF-platelet blood clots.

The identification of this molecular cascade can help scientists better understand the experimental results for the studies of Losartan, Baricitinib, and soluble ACE2 in severe COVID-19 patients (20-22). Losartan was shown to decrease D-dimer, a biomarker for blood clots in elderly COVID-19 patients (20). Baicitinib, a JAK inhibitor, had an 81% mortality benefit in severe COVID-19 patients (21). Soluble ACE2 decreased IL-6 levels in a severe COVID-19 case (22). Soluble ACE2-fC would seem to be the most

viable option for treatment. This drug would not only bind the S1, and covert AngII into Ang-(1-7), but bind SARS-CoV2 virions as well. Alternatively, a combination of Losartan or Baricitinib and Ang-(1-7) could prove to be the best treatment option.

Concluding remarks

The wide range of topics covered in my dissertation research have allowed me to gather a large skill set that will be carried over to my forthcoming postdoctoral position at the University of South Carolina School of Medicine in Dr. Mitzi Nagarkatti's laboratory. I will be working on a variety of topics such as: inflammation, PTSD, the microbiome, and SARS-CoV2 spike phosphorylation which will allow me to use all of the knowledge and skills that I have learned as a graduate student as I continue to grow as a research scientist.

REFERENCES

Chapter 1 References

1. Chibuike GU, Obiora SC. Heavy metal polluted soils: effect on plants and bioremediation methods. Applied and Environmental Soil Science. 2014 Oct;2014.
2. Whitman T, Neurath R, Perera A, Chu-Jacoby I, Ning D, Zhou J, Nico P, Pett-Ridge J, Firestone M. Microbial community assembly differs across minerals in a rhizosphere microcosm. Environmental Microbiology. 2018 Dec;20(12):4444-60.
3. Yang E, Sun L, Ding X, Sun D, Liu J, Wang W. Complete genome sequence of *Caulobacter flavus* RHGG3 T, a type species of the genus *Caulobacter* with plant growth-promoting traits and heavy metal resistance. 3 Biotech. 2019 Feb 1;9(2):42.
4. Poindexter JS. Biological properties and classification of the *Caulobacter* group. Bacteriological Reviews. 1964 Sep;28(3):231.
5. Degnen ST, Newton A. Chromosome replication during development in *Caulobacter crescentus*. Journal of Molecular Biology. 1972 Mar 14;64(3):671-80.

6. Skerker JM, Laub MT. Cell-cycle progression and the generation of asymmetry in *Caulobacter crescentus*. Nature Reviews Microbiology. 2004 Apr;2(4):325-37.
7. Nierman WC, Feldblyum TV, Laub MT, Paulsen IT, Nelson KE, Eisen J, Heidelberg JF, Alley MR, Ohta N, Maddock JR, Potocka I. Complete genome sequence of *Caulobacter crescentus*. Proceedings of the National Academy of Sciences. 2001 Mar 27;98(7):4136-41.
8. Scott D, Ely B. Conservation of the essential genome among *Caulobacter* and *Brevundimonas* species. Current Microbiology. 2016 May 1;72(5):503-10.
9. Ely B, Wilson K, Ross K, Ingram D, Lewter T, Herring J, Duncan D, Aikins A, Scott D. Genome comparisons of wild isolates of *Caulobacter crescentus* reveal rates of inversion and horizontal gene transfer. Current Microbiology. 2019 Feb 15;76(2):159-67.
10. Hanahan D. Studies on transformation of *Escherichia coli* with plasmids. Journal of Molecular Biology. 1983 Jun 5;166(4):557-80.
11. Ash K, Brown T, Watford T, Scott LE, Stephens C, Ely B. A comparison of the *Caulobacter* NA1000 and K31 genomes reveals extensive genome rearrangements and differences in metabolic potential. Open Biology. 2014 Oct 1;4(10):140128.
12. Frost LS, Leplae R, Summers AO, Toussaint A. Mobile genetic elements: the agents of open source evolution. Nature Reviews Microbiology. 2005 Sep;3(9):722-32.
13. Sota M, Top EM. Host-specific factors determine the persistence of IncP-1 plasmids. World Journal of Microbiology and Biotechnology. 2008 Sep 1;24(9):1951-4.

14. Shintani M, Sanchez ZK, Kimbara K. Genomics of microbial plasmids: classification and identification based on replication and transfer systems and host taxonomy. Frontiers in Microbiology. 2015 Mar 31;6:242.
15. Yamaichi Y, Niki H. Active segregation by the *Bacillus subtilis* partitioning system in *Escherichia coli*. Proceedings of the National Academy of Sciences. 2000 Dec 19;97(26):14656-61.
16. Wilhelm RC. Following the terrestrial tracks of *Caulobacter*-redefining the ecology of a reputed aquatic oligotroph. The ISME journal. 2018 Dec;12(12):3025-37.
17. Vodyanitskii YN. Iron hydroxides in soils: a review of publications. Eurasian Soil Science. 2010 Nov 1;43(11):1244-54.
18. Luo D, Langendries S, Mendez SG, De Ryck J, Liu D, Beirinckx S, Willems A, Russinova E, Debode J, Goormachtig S. Plant growth promotion driven by a novel *Caulobacter* strain. Molecular Plant-Microbe Interactions. 2019 Sep 14;32(9):1162-74.
19. Berrios L, Ely B. Plant growth enhancement is not a conserved feature in the *Caulobacter* genus. Plant and Soil. 2020 Mar 2:1-5.
20. Gilchrist AN, Smit JO. Transformation of freshwater and marine Caulobacters by electroporation. Journal of Bacteriology. 1991 Jan 1;173(2):921-5.
21. Smit J, Engelhardt H, Volker S, Smith SH, Baumeister W. The S-layer *of Caulobacter crescentus*: three-dimensional image reconstruction and structure analysis by electron microscopy. Journal of Bacteriology. 1992 Oct 1;174(20):6527-38.

22. Christen B, Abeliuk E, Collier JM, Kalogeraki VS, Passarelli B, Coller JA, Fero MJ, McAdams HH, Shapiro L. The essential genome of a bacterium. Molecular Systems Biology. 2011;7(1):528.
23. Herr KL, Carey AM, Heckman TI, Chávez JL, Johnson CN, Harvey E, Gamroth WA, Wulfing BS, Van Kessel RA, Marks ME. Exopolysaccharide production in *Caulobacter crescentus*: A resource allocation trade-off between protection and proliferation. PLoS One. 2018 Jan 2;13(1):e0190371.
24. Rapkiewicz AV, Mai X, Carsons SE, Pittaluga S, Kleiner DE, Berger JS, Thomas S, Adler NM, Charytan DM, Gasmi B, Hochman JS. Megakaryocytes and platelet-fibrin thrombi characterize multi-organ thrombosis at autopsy in COVID-19: a case series. EClinicalMedicine. 2020 Jul 1.
25. Wichmann D, Sperhake JP, Lütgehetmann M, Steurer S, Edler C, Heinemann A,aHeinrich F, Mushumba H, Kniep I, Schröder AS, Burdelski C. Autopsy findings and venous thromboembolism in patients with COVID-19: a prospective cohort study. Annals of Internal Medicine. 2020 May 6.
26. Lax SF, Skok K, Zechner P, Kessler HH, Kaufmann N, Koelblinger C, Vander K, Bargfrieder U, Trauner M. Pulmonary arterial thrombosis in COVID-19 with fatal outcome: results from a prospective, single-center, clinicopathologic case series. Annals of Internal Medicine. 2020 May 14. doi:10.7326/M20-2566

Chapter 2 References

1. Clowes RC. Molecular structure of bacterial plasmids. Bacteriological Reviews. 1972 Sep;36(3):361.
2. Bouma JE, Lenski RE. Evolution of a bacteria/plasmid association. Nature. 1988 Sep 22;335(6188):351-2.
3. Moreno E. Genome evolution within the alpha Proteobacteria: why do some bacteria not possess plasmids and others exhibit more than one different chromosome? FEMS Microbiology Reviews. 1998 Oct 1;22(4):255-75.
4. Shintani M, Sanchez ZK, Kimbara K. Genomics of microbial plasmids: classification and identification based on replication and transfer systems and host taxonomy. Frontiers in Microbiology. 2015 Mar 31;6:242.
5. Cevallos MA, Cervantes-Rivera R, Gutiérrez-Ríos RM. The *repABC* plasmid family. Plasmid. 2008 Jul 1;60(1):19-37.
6. Pinto UM, Pappas KM, Winans SC. The ABCs of plasmid replication and segregation. Nature Reviews Microbiology. 2012 Nov;10(11):755-65.
7. Poindexter JS. Biological properties and classification of the *Caulobacter* group. Bacteriological Reviews. 1964 Sep;28(3):231.
8. Degnen ST, Newton A. Chromosome replication during development *in Caulobacter crescentus*. Journal of Molecular Biology. 1972 Mar 14;64(3):671-80.
9. Laub MT, McAdams HH, Feldblyum T, Fraser CM, Shapiro L. Global analysis of the genetic network controlling a bacterial cell cycle. Science. 2000 Dec 15;290(5499):2144-8.

10. Ely B. Genetics of *Caulobacter crescentus*. In Methods in Enzymology 1991 Jan 1 (Vol. 204, pp. 372-384). Academic Press.
11. Nierman WC, Feldblyum TV, Laub MT, Paulsen IT, Nelson KE, Eisen J, Heidelberg JF, Alley MR, Ohta N, Maddock JR, Potocka I. Complete genome sequence of *Caulobacter crescentus*. Proceedings of the National Academy of Sciences USA. 2001 Mar 27;98(7):4136-41.
12. Christen B, Abeliuk E, Collier JM, Kalogeraki VS, Passarelli B, Coller JA, Fero MJ, McAdams HH, Shapiro L. The essential genome of a bacterium. Molecular Systems Biology. 2011;7(1):528.
13. Scott D, Ely B. Conservation of the essential genome among *Caulobacter* and *Brevundimonas* species. Current Microbiology. 2016 May 1;72(5):503-10.
14. Ely B, Wilson K, Ross K, Ingram D, Lewter T, Herring J, Duncan D, Aikins A, Scott D. Genome comparisons of wild isolates of *Caulobacter crescentus* reveal rates of inversion and horizontal gene transfer. Current Microbiology. 2019 Feb 15;76(2):159-67.
15. Schoenlein PV, Ely B. Plasmids and bacteriocins in *Caulobacter* species. Journal of Bacteriology. 1983 Feb;153(2):1092.
16. Eberhard WG. Evolution in bacterial plasmids and levels of selection. The Quarterly Review of Biology. 1990 Mar 1;65(1):3-22.
17. Madden T. The BLAST sequence analysis tool. In The NCBI Handbook [Internet]. 2nd edition 2013 Mar 15. National Center for Biotechnology Information (US).
18. Okonechnikov K, Golosova O, Fursov M, Ugene Team. Unipro UGENE: a unified bioinformatics toolkit. Bioinformatics. 2012 Apr 15;28(8):1166-7.

19. Brettin T, Davis JJ, Disz T, Edwards RA, Gerdes S, Olsen GJ, Olson R, Overbeek R, Parrello B, Pusch GD, Shukla M. RASTtk: a modular and extensible implementation of the RAST algorithm for building custom annotation pipelines and annotating batches of genomes. Scientific Reports. 2015 Feb 10;5:8365.
20. Darling AC, Mau B, Blattner FR, Perna NT. Mauve: multiple alignment of conserved genomic sequence with rearrangements. Genome Research. 2004 Jul 1;14(7):1394-403.
21. Johnson RC, Ely B. Isolation of spontaneously derived mutants *of Caulobacter crescentus*. Genetics. 1977 May 1;86(1):25-32.
22. Scott, D., and B. Ely. 2015. Comparison of genome sequencing technology and assembly methods for the analysis of a GC-rich bacterial genome. Current Microbiology 70:338-344.
23. Bartosik D, Szymanik M, Wysocka E. Identification of the partitioning site within the *repABC*-Type Replicon of the composite *Paracoccus versutus* plasmid pTAV1. Journal of Bacteriology. 2001 Nov 1;183(21):6234-43.
24. Wattam AR, Abraham D, Dalay O, Disz TL, Driscoll T, Gabbard JL, Gillespie JJ, Gough R, Hix D, Kenyon R, Machi D. PATRIC, the bacterial bioinformatics database and analysis resource. Nucleic Acids Research. 2014 Jan 1;42(D1):D581-91.
25. Rensing C, Grass G. *Escherichia coli* mechanisms of copper homeostasis in a changing environment. FEMS Microbiology Reviews. 2003 Jun 1;27(2-3):197-213.
26. Arguello JM, Raimunda D, Padilla-Benavides T. Mechanisms of copper homeostasis in bacteria. Frontiers in Cellular and Infection Microbiology. 2013 Nov 5;3:73.

27. Lawton TJ, Kenney GE, Hurley JD, Rosenzweig AC. The CopC family: structural and bioinformatic insights into a diverse group of periplasmic copper binding proteins. Biochemistry. 2016 Apr 19;55(15):2278-90.
28. Blair JM, Piddock LJ. Structure, function and inhibition of RND efflux pumps in Gram-negative bacteria: an update. Current Opinion in Microbiology. 2009 Oct 1;12(5):512-9.
29. Inesi G, Pilankatta R, Tadini-Buoninsegni F. Biochemical characterization of P-type copper ATPases. Biochemical Journal. 2014 Oct 15;463(2):167-76.
30. Giachino A, Waldron KJ. Copper tolerance in bacteria requires the activation of multiple accessory pathways. Molecular Microbiology. 2020 Apr 23.
31. Fang C, Philips SJ, Wu X, Chen K, Shi J, Shen L, Xu J, Feng Y, O'Halloran TV, Zhang Y. CueR activates transcription through a DNA distortion mechanism. Nature Chemical Biology. 2020 Sep 28:1-8.
32. Moraleda-Muñoz A, Pérez J, Extremera AL, Muñoz-Dorado J. Differential regulation of six heavy metal efflux systems in the response of *Myxococcus xanthus* to copper. Applied and Environmental Microbiology. 2010 Sep 15;76(18):6069-76.
33. Hassan KA, Pederick VG, Elbourne LD, Paulsen IT, Paton JC, McDevitt CA, Eijkelkamp BA. Zinc stress induces copper depletion in *Acinetobacter baumannii*. BMC microbiology. 2017 Dec;17(1):1-5.
34. Solioz M, Odermatt A. Copper and silver transport by CopB-ATPase in membrane vesicles of *Enterococcus hirae*. Journal of Biological Chemistry. 1995 Apr 21;270(16):9217-21.

35. Crack JC, Green J, Hutchings MI, Thomson AJ, Le Brun NE. Bacterial iron–sulfur regulatory proteins as biological sensor-switches. Antioxidants & Redox Signaling. 2012 Nov 1;17(9):1215-31.
36. Stoyanov JV, Hobman JL, Brown NL. CueR (YbbI) of *Escherichia coli* is a MerR family regulator controlling expression of the copper exporter CopA. Molecular Microbiology. 2001 Jan;39(2):502-12.
37. Outten FW, Outten CE, Hale J, O'Halloran TV. Transcriptional activation of an *Escherichia coli* copper efflux regulon by the chromosomal MerR homologue, CueR. Journal of Biological Chemistry. 2000 Oct 6;275(40):31024-9.
38. Whitman T, Neurath R, Perera A, Chu-Jacoby I, Ning D, Zhou J, Nico P, Pett-Ridge J, Firestone M. Microbial community assembly differs across minerals in a rhizosphere microcosm. Environmental microbiology. 2018 Dec;20(12):4444-60.
39. Gupta P, Diwan B. Bacterial exopolysaccharide mediated heavy metal removal: a review on biosynthesis, mechanism and remediation strategies. Biotechnology Reports. 2017 Mar 1;13:58-71.
40. Qi X, Liu R, Chen M, Li Z, Qin T, Qian Y, Zhao S, Liu M, Zeng Q, Shen J. Removal of copper ions from water using polysaccharide-constructed hydrogels. Carbohydrate Polymers. 2019 Apr 1;209:101-10.
41. Deschatre M, Ghillebaert F, Guezennec J, Colin CS. Sorption of copper (II) and silver (I) by four bacterial exopolysaccharides. Applied Biochemistry and Biotechnology. 2013 Nov 1;171(6):1313-27.

42. Vodyanitskii YN. Iron hydroxides in soils: a review of publications. Eurasian Soil Science. 2010 Nov 1;43(11):1244-54.

Chapter 3 References

1. Skerker JM, Laub MT. Cell-cycle progression and the generation of asymmetry in *Caulobacter crescentus*. Nature Reviews Microbiology. 2004 Apr;2(4):325-37.
2. Ely B. Genetics of *Caulobacter crescentus*. In Methods in Enzymology 1991 Jan 1 (Vol. 204, pp. 372-384). Academic Press.
3. Nierman WC, Feldblyum TV, Laub MT, Paulsen IT, Nelson KE, Eisen J, Heidelberg JF, Alley MR, Ohta N, Maddock JR, Potocka I. Complete genome sequence of *Caulobacter crescentus*. Proceedings of the National Academy of Sciences. 2001 Mar 27;98(7):4136-41.
4. Govers SK, Jacobs-Wagner C. *Caulobacter crescentus*: model system extraordinaire. Current Biology. 2020 Oct 5;30(19):R1151-8.
5. Schoenlein PV, Ely B. Plasmids and bacteriocins in *Caulobacter* species. Journal of Bacteriology. 1983 Feb;153(2):1092.
6. Poindexter JS. Biological properties and classification of the *Caulobacter* group. Bacteriological Reviews. 1964 Sep;28(3):231.
7. Scott D, Ely B. Conservation of the essential genome among *Caulobacter* and *Brevundimonas* species. Current Microbiology. 2016 May 1;72(5):503-10.

8. Christen B, Abeliuk E, Collier JM, Kalogeraki VS, Passarelli B, Coller JA, Fero MJ, McAdams HH, Shapiro L. The essential genome of a bacterium. Molecular Systems Biology. 2011;7(1):528.
9. Gilchrist AN, Smit JO. Transformation of freshwater and marine Caulobacters by electroporation. Journal of Bacteriology. 1991 Jan 1;173(2):921-5.
10. Herr KL, Carey AM, Heckman TI, Chávez JL, Johnson CN, Harvey E, Gamroth WA, Wulfing BS, Van Kessel RA, Marks ME. Exopolysaccharide production in *Caulobacter crescentus*: A resource allocation trade-off between protection and proliferation. PLoS One. 2018 Jan 2;13(1):e0190371.
11. Smit J, Engelhardt H, Volker S, Smith SH, Baumeister W. The S-layer of *Caulobacter crescentus*: three-dimensional image reconstruction and structure analysis by electron microscopy. Journal of Bacteriology. 1992 Oct 1;174(20):6527-38.
12. Walker SG, Smith SH, Smit J. Isolation and comparison of the paracrystalline surface layer proteins of freshwater Caulobacters. Journal of Bacteriology. 1992 Mar 1;174(6):1783-92.
13. Sleytr UB, Beveridge TJ. Bacterial S-layers. Trends in Microbiology. 1999 Jun 1;7(6):253-60.
14. Herrmann J, Jabbarpour F, Bargar PG, Nomellini JF, Li PN, Lane TJ, Weiss TM, Smit J, Shapiro L, Wakatsuki S. Environmental calcium controls alternate physical states of the *Caulobacter* surface layer. Biophysical Journal. 2017 May 9;112(9):1841-51.
15. Walker DC, Aoyama K, Klaenhammer TR. Electrotransformation of Lactobacillus acidophilus group A1. FEMS microbiology letters. 1996 May 1;138(2-3):233-7.

16. Hermans J, Boschloo JG, De Bont JA. Transformation of Mycobacterium aurum by electroporation: the use of glycine, lysozyme and isonicotinic acid hydrazide in enhancing transformation efficiency. FEMS Microbiology Letters. 1990 Oct 1;72(1-2):221-4.
17. Holo H, Nes IF. High-frequency transformation, by electroporation, of *Lactococcus lactis* subsp. cremoris grown with glycine in osmotically stabilized media. Applied and Environmental Microbiology. 1989 Dec 1;55(12):3119-23.
18. Spath K, Heinl S, Grabherr R. Direct cloning in *Lactobacillus plantarum*: electroporation with non-methylated plasmid DNA enhances transformation efficiency and makes shuttle vectors obsolete. Microbial Cell Factories. 2012 Dec;11(1):1-8.
19. Singh M, Yadav A, Ma X, Amoah E. Plasmid DNA transformation in *Escherichia coli*: effect of heat shock temperature, duration, and cold incubation of CaCl2 treated cells. International Journal of Biotechnology and Biochemistry. 2010;6(4):561-8.
20. Bertani G. Studies on lysogenesis I.: the mode of phage liberation by lysogenic *Escherichia coli*. Journal of Bacteriology. 1951 Sep;62(3):293.
21. Ely B. Genetics of *Caulobacter crescentus*. In Methods in Enzymology 1991 Jan 1 (Vol. 204, pp. 372-384). Academic Press.
22. Fournet-Fayard S, Joly B, Forestier C. Transformation of wild *type Klebsiella pneumoniae* with plasmid DNA by electroporation. Journal of Microbiological Methods. 1995 Nov 1;24(1):49-54.
23. Ely B, Johnson RC. Generalized transduction in Caulobacter crescentus. Genetics. 1977 Nov 30;87(3):391-9.

24. Ely B. Transfer of drug resistance factors to the dimorphic bacterium *Caulobacter crescentus*. Genetics. 1979 Mar 1;91(3):371-80.
25. O'Neill EA, Berlinberg C, Bender RA. Activity of plasmid replicons in *Caulobacter crescentus*: RP4 and ColE1. Genetics. 1983 Apr 1;103(4):593-604.

Chapter 4 References

1. Centers for Disease Control and Prevention. Coronavirus disease 2019. Cumulative total number of COVID-19 cases in the United States by report date, January 12, 2020 to November 21, 2020. https://www.cdc.gov/coronavirus/2019-ncov/cases-updates/cases-in-us.html#cumulative Accessed November 22, 2020.
2. Rapkiewicz AV, Mai X, Carsons SE, Pittaluga S, Kleiner DE, Berger JS, Thomas S, Adler NM, Charytan DM, Gasmi B, Hochman JS. Megakaryocytes and platelet-fibrin thrombi characterize multi-organ thrombosis at autopsy in COVID-19: a case series. EClinicalMedicine. 2020 Jul 1.. doi.org/10.1016/j.eclinm.2020.100434
3. Wichmann D, Sperhake JP, Lütgehetmann M, Steurer S, Edler C, Heinemann A, Heinrich F, Mushumba H, Kniep I, Schröder AS, Burdelski C. Autopsy findings and venous thromboembolism in patients with COVID-19: a prospective cohort study. Annals of internal medicine. 2020 May 6. doi.org/10.7326/M20-2003
4. Lax SF, Skok K, Zechner P, Kessler HH, Kaufmann N, Koelblinger C, Vander K, Bargfrieder U, Trauner M. Pulmonary arterial thrombosis in COVID-19 with fatal outcome: results from a prospective, single-center, clinicopathologic case series. Annals of Internal Medicine. 2020 May 14. doi:10.7326/M20-2566

5. Li W, Moore MJ, Vasilieva N, Sui J, Wong SK, Berne MA, Somasundaran M, Sullivan JL, Luzuriaga K, Greenough TC, Choe H. Angiotensin-converting enzyme 2 is a functional receptor for the SARS coronavirus. Nature. 2003 Nov;426(6965):450-4
6. Hoffmann M, Kleine-Weber H, Schroeder S, Krüger N, Herrler T, Erichsen S, Schiergens TS, Herrler G, Wu NH, Nitsche A, Müller MA. SARS-CoV-2 cell entry depends on ACE2 and TMPRSS2 and is blocked by a clinically proven protease inhibitor. Cell. 2020 Mar 5. doi.org/10.1016/j.cell.2020.02.052
7. AC, Park YJ, Tortorici MA, Wall A, McGuire AT, Veesler D. Structure, function, and antigenicity of the SARS-CoV-2 spike glycoprotein. Cell. 2020 Mar 9. doi.org/10.1016/j.cell.2020.02.058
8. Thomas G. Furin at the cutting edge: from protein traffic to embryogenesis and disease. Nature reviews Molecular cell biology. 2002 Oct;3(10):753-66.
9. Shang J, Wan Y, Luo C, Ye G, Geng Q, Auerbach A, Li F. Cell entry mechanisms of SARS-CoV-2. Proceedings of the National Academy of Sciences. 2020 May 26. doi.org/10.1073/pnas.2003138117
10. Gierer S, Müller MA, Heurich A, Ritz D, Springstein BL, Karsten CB, Schendzielorz A, Gnirß K, Drosten C, Pöhlmann S. Inhibition of proprotein convertases abrogates processing of the middle eastern respiratory syndrome coronavirus spike protein in infected cells but does not reduce viral infectivity. The Journal of infectious diseases. 2015 Mar 15; 211(6):889-97.

11. Gordon DE, Jang GM, Bouhaddou M, Xu J, Obernier K, White KM, O'Meara MJ, Rezelj VV, Guo JZ, Swaney DL, Tummino TA. A SARS-CoV-2 protein interaction map reveals targets for drug repurposing. Nature. 2020 Apr 30. doi.org/10.1038/s41586-020-2286-9
12. Petroski MD, Deshaies RJ. Function and regulation of cullin–RING ubiquitin ligases. Nature reviews Molecular cell biology. 2005 Jan;6(1):9-20.
13. Tan CW, Chia WN, Qin X, Liu P, Chen MI, Tiu C, Hu Z, Chen VC, Young BE, Sia WR, Tan YJ. A SARS-CoV-2 surrogate virus neutralization test based on antibody-mediated blockage of ACE2–spike protein–protein interaction. Nature biotechnology. 2020 Jul 23. doi.org/10.1038/s41587-020-0631-z
14. Cai Y, Zhang J, Xiao T, Peng H, Sterling SM, Walsh RM, et al. Distinct conformational states of SARS-CoV-2 spike protein. Science. 2020 Sep 21. doi.org/10.1126/science.abd4251
15. Zhao X, Chen D, Szabla R, Zheng M, Li G, Du P et al. Broad and Differential Animal Angiotensin-Converting Enzyme 2 Receptor Usage by SARS-CoV-2. Journal of Virology. 2020;94(18).
16. Oudit GY, Zhong J, Basu R, Guo D, Penninger JM, Kassiri Z. Angiotensin Converting Enzyme 2 Suppresses Pathological Hypertrophy, Myocardial Fibrosis and Diastolic Dysfunction. Journal of Cardiac Failure. 2010 Aug 1;16(8):S16.
17. Givertz MM. Manipulation of the renin-angiotensin system. Circulation. 2001 Jul 31;104(5):e14-8.
18. Lee MA, Böhm M, Paul M, Ganten D. Tissue renin-angiotensin systems. Their role in cardiovascular disease. Circulation. 1993 May;87(5 Suppl):IV7.

19. Murphy TJ, Alexander RW, Griendling KK, Runge MS, Bernstein KE. Isolation of a cDNA encoding the vascular type-1 angiotensin II receptor. Nature. 1991 May;351(6323):233-6
20. Horiuchi M, Akishita M, Dzau VJ. Recent progress in angiotensin II type 2 receptor research in the cardiovascular system. Hypertension. 1999 Feb;33(2):613-21.
21. Santos RA, e Silva AC, Maric C, Silva DM, Machado RP, de Buhr I, Heringer-Walther S, Pinheiro SV, Lopes MT, Bader M, Mendes EP. Angiotensin-(1–7) is an endogenous ligand for the G protein-coupled receptor Mas. Proceedings of the National Academy of Sciences. 2003 Jul 8;100(14):8258-63.
22. Kuba K, Imai Y, Penninger JM. Multiple functions of angiotensin-converting enzyme 2 and its relevance in cardiovascular diseases. Circulation Journal. 2013;77(2):301-8.
23. Wu Z, Hu R, Zhang C, Ren W, Yu A, Zhou X. Elevation of plasma angiotensin II level is a potential pathogenesis for the critically ill COVID-19 patients. Critical Care. 2020 Dec;24(1):1-3.
24. Han Y, Runge MS, Brasier AR. Angiotensin II induces interleukin-6 transcription in vascular smooth muscle cells through pleiotropic activation of nuclear factor-κB transcription factors. Circulation research. 1999 Apr 2;84(6):695-703.
25. Clancy P, Koblar SA, Golledge J. Angiotensin receptor 1 blockade reduces secretion of inflammation associated cytokines from cultured human carotid atheroma and vascular cells in association with reduced extracellular signal regulated kinase expression and activation. Atherosclerosis. 2014 Sep 1;236(1):108-15.

26. Schrader LI, Kinzenbaw DA, Johnson AW, Faraci FM, Didion SP. IL-6 deficiency protects against angiotensin II–induced endothelial dysfunction and hypertrophy. Arteriosclerosis, thrombosis, and vascular biology. 2007 Dec 1;27(12):2576-81.
27. Zhang W, Wang W, Yu H, Zhang Y, Dai Y, Ning C, Tao L, Sun H, Kellems RE, Blackburn MR, Xia Y. Interleukin 6 underlies angiotensin II–induced hypertension and chronic renal damage. Hypertension. 2012 Jan;59(1):136-44.
28. Wassmann S, Stumpf M, Strehlow K, Schmid A, Schieffer B, Böhm M, Nickenig G. Interleukin-6 induces oxidative stress and endothelial dysfunction by overexpression of the angiotensin II type 1 receptor. Circulation research. 2004 Mar 5;94(4):534-41.
29. Souza LL, Costa-Neto CM. Angiotensin-(1–7) decreases LPS-induced inflammatory response in macrophages. Journal of cellular physiology. 2012 May;227(5):2117-22.
30. Chen X, Zhao B, Qu Y, Chen Y, Xiong J, Feng Y, Men D, Huang Q, Liu Y, Yang B, Ding J. Detectable serum SARS-CoV-2 viral load (RNAaemia) is closely correlated with drastically elevated interleukin 6 (IL-6) level in critically ill COVID-19 patients. Clinical Infectious Diseases. 2020 Apr 17. doi.org/10.1093/cid/ciaa449
31. Italiano Jr JE, Shivdasani RA. Megakaryocytes and beyond: the birth of platelets. Journal of Thrombosis and Haemostasis. 2003 Jun;1(6):1174-82.
32. Kaufman RM, Airo R, Pollack S, Crosby WH. Circulating megakaryocytes and platelet release in the lung. Blood. 1965 Dec;26(6):720-31.
33. Wei SG, Zhang ZH, Yu Y, Felder RB. Central SDF-1/CXCL12 expression and its cardiovascular and sympathetic effects: the role of angiotensin II, TNF-α, and MAP

kinase signaling. American Journal of Physiology-Heart and Circulatory Physiology. 2014 Dec 1;307(11):H1643-54.

34. Amano H, Ito Y, Ogawa F, Eshima K, Suzuki T, Oba K, Matsui Y, Kato S, Fukui T, Nakamura M, Kitasato H. Angiotensin II type 1A receptor signaling facilitates tumor metastasis formation through P-selectin–Mediated interaction of tumor cells with platelets and endothelial cells. The American journal of pathology. 2013 Feb 1;182(2):553-64.
35. Hamada T, Möhle R, Hesselgesser J, Hoxie J, Nachman RL, Moore MA, Rafii S. Transendothelial migration of megakaryocytes in response to stromal cell-derived factor 1 (SDF-1) enhances platelet formation. The Journal of experimental medicine. 1998 Aug 3;188(3):539-48.
36. Lane WJ, Dias S, Hattori K, Heissig B, Choy M, Rabbany SY, Wood J, Moore MA, Rafii S. Stromal-derived factor 1–induced megakaryocyte migration and platelet production is dependent on matrix metalloproteinases. Blood, The Journal of the American Society of Hematology. 2000 Dec 15;96(13):4152-9.
37. Kaser A, Brandacher G, Steurer W, Kaser S, Offner FA, Zoller H, Theurl I, Widder W, Molnar C, Ludwiczek O, Atkins MB. Interleukin-6 stimulates thrombopoiesis through thrombopoietin: role in inflammatory thrombocytosis. Blood, The Journal of the American Society of Hematology. 2001 Nov 1;98(9):2720-5.
38. Kaushansky K. Thrombopoietin. New England Journal of Medicine. 1998 Sep 10;339(11):746-54.
39. Siddiqui FA, Desai H, Amirkhosravi A, Amaya M, Francis JL. The presence and release of tissue factor from human platelets. Platelets. 2002 Jan 1;13(4):247-53.

40. Hottz ED, Azevedo-Quintanilha IG, Palhinha L, Teixeira L, Barreto EA, Pão CR, Righy C, Franco S, Souza TM, Kurtz P, Bozza FA. Platelet activation and platelet-monocyte aggregate formation trigger tissue factor expression in patients with severe COVID-19. Blood, The Journal of the American Society of Hematology. 2020 Sep 10;136(11):1330-41.

41. Skendros P, Mitsios A, Chrysanthopoulou A, Mastellos DC, Metallidis S, Rafailidis P, Ntinopoulou M, Sertaridou E, Tsironidou V, Tsigalou C, Tektonidou MG. Complement and tissue factor-enriched neutrophil extracellular traps are key drivers in COVID-19 immunothrombosis. The Journal of Clinical Investigation. 2020 Aug 6. doi.org/10.1172/JCI141374

42. Gould TJ, Vu TT, Swystun LL, Dwivedi DJ, Mai SH, Weitz JI, Liaw PC. Neutrophil extracellular traps promote thrombin generation through platelet-dependent and platelet-independent mechanisms. Arteriosclerosis, thrombosis, and vascular biology. 2014 Sep;34(9):1977-84.

43. Zuo Y, Yalavarthi S, Shi H, Gockman K, Zuo M, Madison JA, et al. Neutrophil extracellular traps in COVID-19. JCI Insight. 2020; doi.org/10.1172/jci.insight.138999

44. Nabah YN, Mateo T, Estellés R, Mata M, Zagorski J, Sarau H, Cortijo J, Morcillo EJ, Jose PJ, Sanz MJ. Angiotensin II induces neutrophil accumulation in vivo through generation and release of CXC chemokines. Circulation. 2004 Dec 7;110(23):3581-6.

45. Brambilla M, Gelosa P, Rossetti L, Castiglioni L, Zara C, Canzano P, Tremoli E, Sironi L, Camera M. Impact of angiotensin-converting enzyme inhibition on platelet tissue factor expression in stroke-prone rats. Journal of Hypertension. 2018 Jun;36(6):1360.

46. Jagroop IA, Mikhailidis DP. Angiotensin II can induce and potentiate shape change in human platelets: effect of losartan. Journal of human hypertension. 2000 Sep;14(9):581-5.

47. Buja LM, Wolf D, Zhao B, Akkanti B, McDonald M, Lelenwa L, Reilly N, Ottaviani G, Elghetany MT, Trujillo DO, Aisenberg GM. Emerging spectrum of cardiopulmonary pathology of the coronavirus disease 2019 (COVID-19): Report of three autopsies from Houston, Texas and review of autopsy findings from other United States cities. Cardiovascular Pathology. 2020 May 7. doi.org/10.1016/j.carpath.2020.107233

48. Chen J, Jiang Q, Xia X, Liu K, Yu Z, Tao W, Gong W, Han JD. Individual variation of the SARS-CoV-2 receptor ACE2 gene expression and regulation. Aging cell. 2020 Jul;19(7). doi.org/10.1111/acel.13168

49. Wang Z, Yang X, Zhou Y, Sun J, Liu X, Zhang J, Mei X, Zhong J, Zhao J, Ran P. COVID-19 Severity Correlates with Weaker T-Cell Immunity, Hypercytokinemia, and Lung Epithelium Injury. American Journal of Respiratory and Critical Care Medicine. 2020 Aug 15;202(4):606-10.

50. Teng YH, Aquino RS, Park PW. Molecular functions of syndecan-1 in disease. Matrix biology. 2012 Jan 1;31(1):3-16.

51. Wang W, Haller CA, Wen J, Wang P, Chaikof EL. Decoupled syndecan 1 mRNA and protein expression is differentially regulated by angiotensin II in macrophages. Journal of cellular physiology. 2008 Mar;214(3):750-6.

52. Schellings MW, Vanhoutte D, van Almen GC, Swinnen M, Leenders JJ, Kubben N, van Leeuwen RE, Hofstra L, Heymans S, Pinto YM. Syndecan-1 amplifies angiotensin II–induced cardiac fibrosis. Hypertension. 2010 Feb 1;55(2):249-56.

53. Yan F, Huang F, Xu J, Yang P, Qin Y, Lv J, Zhang S, Ye L, Gong M, Liu Z, Wei J. Antihypertensive drugs are associated with reduced fatal outcomes and improved clinical characteristics in elderly COVID-19 patients. Cell Discovery. 2020 Oct 29;6(1):1-0.

54. Goldberg AI, Dunlay MC, Sweet CS. Safety and tolerability of losartan potassium, an angiotensin II receptor antagonist, compared with hydrochlorothiazide, atenolol, felodipne ER, and angiotensin-converting enzyme inhibitors for the treatment of systemic hypertension. The American journal of cardiology. 1995 Apr 15;75(12):793-5.

55. Axelsson A, Iversen K, Vejlstrup N, Ho C, Norsk J, Langhoff L, Ahtarovski K, Corell P, Havndrup O, Jensen M, Bundgaard H. Efficacy and safety of the angiotensin II receptor blocker losartan for hypertrophic cardiomyopathy: the INHERIT randomised, double-blind, placebo-controlled trial. The Lancet Diabetes & Endocrinology. 2015 Feb 1;3(2):123-31.

56. Stebbing J, Nievas GS, Falcone M, Youhanna S, Richardson P, Ottaviani S, Shen JX, Sommerauer C, Tiseo G, Ghiadoni L, Virdis A. JAK inhibition reduces SARS-CoV-2 liver infectivity and modulates inflammatory responses to reduce morbidity and mortality. Science Advances. 2020 Nov 13:eabe4724.

57. Satou R, Gonzalez-Villalobos RA. JAK-STAT and the renin-angiotensin system: The role of the JAK-STAT pathway in blood pressure and intrarenal renin-angiotensin system regulation. Jak-stat. 2012 Oct 1;1(4):250-6.

58. Smolen JS, Genovese MC, Takeuchi T, Hyslop DL, Macias WL, Rooney T, Chen L, Dickson CL, Camp JR, Cardillo TE, Ishii T. Safety profile of baricitinib in patients with active rheumatoid arthritis with over 2 years median time in treatment. The Journal of Rheumatology. 2019 Jan 1;46(1):7-18.
59. Zoufaly A, Poglitsch M, Aberle JH, Hoepler W, Seitz T, Traugott M, Grieb A, Pawelka E, Laferl H, Wenisch C, Neuhold S. Human recombinant soluble ACE2 in severe COVID-19. The Lancet Respiratory Medicine. 2020 Nov 1;8(11):1154-8.
60. Ke Z, Oton J, Qu K, Cortese M, Zila V, McKeane L, Nakane T, Zivanov J, Neufeldt CJ, Cerikan B, Lu JM. Structures and distributions of SARS-CoV-2 spike proteins on intact virions. Nature. 2020 Aug 17:1-5.

Chapter 5 References

1. Gaddy L, Carter T, Ely B, Sakaguchi S, Matsuo A, Suyama Y. *Shortia brevistyla* comb. et stat. nov. Diapensiaceae), a narrow endemic from the headwaters of the Catawba River in North Carolina, USA Phytologia. 2019;101:113-9.
2. Scott D, Ely B. Conservation of the essential genome among *Caulobacter* and *Brevundimonas* species. Current Microbiology. 2016 May 1;72(5):503-10.
3. Ely B, Wilson K, Ross K, Ingram D, Lewter T, Herring J, Duncan D, Aikins A, Scott D. Genome comparisons of wild isolates of *Caulobacter crescentus* reveal rates of inversion and horizontal gene transfer. Current Microbiology. 2019 Feb 15;76(2):159-67.

4. Shintani M, Sanchez ZK, Kimbara K. Genomics of microbial plasmids: classification and identification based on replication and transfer systems and host taxonomy. Frontiers in Microbiology. 2015 Mar 31;6:242.
5. Whitman T, Neurath R, Perera A, Chu-Jacoby I, Ning D, Zhou J, Nico P, Pett-Ridge J, Firestone M. Microbial community assembly differs across minerals in a rhizosphere microcosm. Environmental Microbiology. 2018 Dec;20(12):4444-60.
6. Vodyanitskii YN. Iron hydroxides in soils: a review of publications. Eurasian Soil Science. 2010 Nov 1;43(11):1244-54.
7. Gupta P, Diwan B. Bacterial exopolysaccharide mediated heavy metal removal: a review on biosynthesis, mechanism and remediation strategies. Biotechnology Reports. 2017 Mar 1;13:58-71.
8. Qi X, Liu R, Chen M, Li Z, Qin T, Qian Y, Zhao S, Liu M, Zeng Q, Shen J. Removal of copper ions from water using polysaccharide-constructed hydrogels. Carbohydrate Polymers. 2019 Apr 1;209:101-10.
9. Gilchrist AN, Smit JO. Transformation of freshwater and marine Caulobacters by electroporation. Journal of Bacteriology. 1991 Jan 1;173(2):921-5.
10. Walker DC, Aoyama K, Klaenhammer TR. Electrotransformation of *Lactobacillus acidophilus* group A1. FEMS Microbiology Letters. 1996 May 1;138(2-3):233-7.
11. Hermans J, Boschloo JG, De Bont JA. Transformation of *Mycobacterium aurum* by electroporation: the use of glycine, lysozyme and isonicotinic acid hydrazide in enhancing transformation efficiency. FEMS Microbiology Letters. 1990 Oct 1;72(1-2):221-4.

12. Holo H, Nes IF. High-frequency transformation, by electroporation, *of Lactococcus lactis* subsp. cremoris grown with glycine in osmotically stabilized media. Applied and Environmental Microbiology. 1989 Dec 1;55(12):3119-23.
13. Herr KL, Carey AM, Heckman TI, Chávez JL, Johnson CN, Harvey E, Gamroth WA, Wulfing BS, Van Kessel RA, Marks ME. Exopolysaccharide production in *Caulobacter crescentus*: A resource allocation trade-off between protection and proliferation. PLoS One. 2018 Jan 2;13(1):e0190371.
14. Fournet-Fayard S, Joly B, Forestier C. Transformation of wild type *Klebsiella pneumoniae* with plasmid DNA by electroporation. Journal of Microbiological Methods. 1995 Nov 1;24(1):49-54.
15. Herrmann J, Jabbarpour F, Bargar PG, Nomellini JF, Li PN, Lane TJ, Weiss TM, Smit J, Shapiro L, Wakatsuki S. Environmental calcium controls alternate physical states of the *Caulobacter* surface layer. Biophysical Journal. 2017 May 9;112(9):1841-51.
16. Rapkiewicz AV, Mai X, Carsons SE, Pittaluga S, Kleiner DE, Berger JS, Thomas S, Adler NM, Charytan DM, Gasmi B, Hochman JS. Megakaryocytes and platelet-fibrin thrombi characterize multi-organ thrombosis at autopsy in COVID-19: a case series. EClinicalMedicine. 2020 Jul 1..
17. Wichmann D, Sperhake JP, Lütgehetmann M, Steurer S, Edler C, Heinemann A,Heinrich F, Mushumba H, Kniep I, Schröder AS, Burdelski C. Autopsy findings and venous thromboembolism in patients with COVID-19: a prospective cohort study. Annals of Internal Medicine. 2020 May 6.

18. Lax SF, Skok K, Zechner P, Kessler HH, Kaufmann N, Koelblinger C, Vander K, Bargfrieder U, Trauner M. Pulmonary arterial thrombosis in COVID-19 with fatal outcome: results from a prospective, single-center, clinicopathologic case series. Annals of Internal Medicine. 2020 May 14. doi:10.7326/M20-2566
19. Paul M, Poyan Mehr A, Kreutz R. Physiology of local renin-angiotensin systems. Physiological Reviews. 2006 Jul;86(3):747-803.
20. Yan F, Huang F, Xu J, Yang P, Qin Y, Lv J, Zhang S, Ye L, Gong M, Liu Z, Wei J. Antihypertensive drugs are associated with reduced fatal outcomes and improved clinical characteristics in elderly COVID-19 patients. Cell Discovery. 2020 Oct 29;6(1):1-0.
21. Stebbing J, Nievas GS, Falcone M, Youhanna S, Richardson P, Ottaviani S, Shen JX, Sommerauer C, Tiseo G, Ghiadoni L, Virdis A. JAK inhibition reduces SARS-CoV-2 liver infectivity and modulates inflammatory responses to reduce morbidity and mortality. Science Advances. 2020 Nov 13:eabe4724.
22. Zoufaly A, Poglitsch M, Aberle JH, Hoepler W, Seitz T, Traugott M, Grieb A, Pawelka E, Laferl H, Wenisch C, Neuhold S. Human recombinant soluble ACE2 in severe COVID-19. The Lancet Respiratory Medicine. 2020 Nov 1;8(11):1154-8.

APPENDIX A

THE CORONAVIRUS GENOME IS LIKE A SHIPPING LABEL THAT LETS EPIDEMIOLOGISTS TRACK WHERE IT'S BEEN

Ely, B and Carter, T. Coversation.org. 2020. Creative Commons

Following the coronavirus's spread through the population – and anticipating its next move – is an important part of the public health response to the new disease, especially since containment is our only defense so far. Just looking at an infected person doesn't tell you where their version of the coronavirus came from, and SARS-CoV-2 doesn't have a bar code you can scan to allow you to track its travel history. However, its genetic sequence is almost as good for providing some insight into where the virus has been.

An organism's genome is its complete genetic instructions. You can think of a genome as a book, containing words made up of letters. Each "letter" in the genome is a molecule called a nucleotide – in shorthand, an A, G, C, T or U. Mutations can occur every time the virus replicates its genome, so that over time mutations accumulate in the viral genome. For example, in place of the "word" CAT, the new virus has GAT. The virus carries these minor modifications as it moves from one person to the next host. These mutations behave like a passport stamp. No matter where you go next, previous stamps in your passport still show where you've been.

Molecular geneticists like us can use this information to construct family trees for the coronavirus. That allows us to trace the routes the virus has traveled through space and time and start to answer questions like how quickly and easily does it spread from one person to another?

Individual patient data help paint a big picture

Online databases have been collecting SARS-CoV-2 genomic nucleotide sequences since mid December. Whenever a patient tests positive for SARS-CoV-2, a lab

can determine the genome sequence of the infecting virus and upload it. As of late April, more than 1,500 genome sequence samples have been deposited in GenBank, a publicly available database run by the National Institutes of Health, and more than 13,000 are in GISAID, the open-access Global Initiative on Sharing All Influenza Data.

Since each sequence is from a patient who is in a specific place in the world, these viral genome sequences allow scientists to compare them and track where the virus has been. The more similar the sequences from two particular viruses are, the more closely related they are and the more recently they've shared a common ancestor. The first SARS-CoV-2 genomic sequence uploaded to the GISAID's website was collected from a patient in early December 2019.

Of course, the viral mutations themselves do not tell researchers which country they happened in. But since the databases record where particular patterns of mutations have been observed, scientists can determine the route that each viral strain has taken. The global map tracks the movement of the virus around the world. The data recorded from thousands of patients show that SARS-Cov-2 originated in Wuhan China and spread from there to the rest of the world.

The SARS-CoV-2 phylogenetic tree – the family tree that connects all the sequenced coronavirus samples worldwide. The colors denote regional 'branches' of the tree. nextstrain.org, CC BY

Building maps out of sequences

The genetic data can play a big role in cracking public health mysteries, like how the coronavirus has spread through the United States. For example, a traveler from Wuhan arrived in Seattle on Jan. 15 and tested positive for the virus on Jan. 20.

On Feb. 28, scientists sequenced a virus sample from an American patient in Seattle and found its mutation signature matched that of the virus from the Wuhan traveler, plus three new mutations. GISAID has estimated the mutation rate at about 0.45 mutations per genome per week – so three mutations between the Jan. 20 case and the Feb. 28 case fits that rate.

Based on the three new mutations, this version of the virus had been multiplying undetected for about five weeks in the Seattle area. Since each infected person can infect several other people without experiencing any symptoms themselves, the virus could have spread to more than 100 people in five weeks.

Using the genome sequences to link the virus from the Jan. 15 traveler from Wuhan with the Washington-based patient from the end of February alerted Washington state officials that the virus was silently spreading through the population. This undetected spreading of the virus in Seattle and elsewhere is one of the primary reasons public health officials are calling for the public to stay home as much as possible.

Another study detailed the path the virus took as it moved from Wuhan to Shanghai to Germany to Italy to Mexico, stowing away in infected travelers. This study

tracked infected individuals and compared their viral genomic sequences. Since researchers could compare the viral mutations to those in known locations at specific times, they were able to map out the phylogenetic tree – the family tree that shows how the various virus genome sequences are related.

Using the GISAID estimated mutation rate and the phylogenetic tree, scientists think the first time the coronavirus infected a person likely occurred in Wuhan in November or early December 2019.

If the virus had been around much longer, the viruses of the first known patients would have had a larger variety of mutations than they did.

Still tracking and learning from the sequences

The analysis of viral genomic sequences will continue to be a valuable tool for tracking and containing the spread of SARS-CoV-2.

For instance, sequencing the genome of a virus from a newly infected patient could tell you if it is a virus that has been circulating in the area for a while, or if it is a new introduction from elsewhere.

Someone who'd been in northern Italy before travel restrictions were in place brought the virus to Iceland. That initial outbreak was contained fairly quickly, but then new forms of the virus were introduced from elsewhere in Europe.

A new study pending peer-review indicates that California also had multiple introduction events with distinct viral lineages. For California, knowledge of the

frequency of new introductions would be an important factor to consider as officials devise ways to contain the virus.

Viral genome sequences can be informative in other ways as well. Eventually, researchers may find that some forms of the virus are more virulent than others. In that case, the sequence of the viral genome could help physicians decide which treatment would be best for a particular patient.

APPENDIX B

CHAPTER 2 SUPPLEMENTARY TABLES

Table B.1. qPCR primer list.

1. Heavy metal translocating P-type ATPase (895, 2931)
   F: GCCTTTGAGCCTGTTTATCATC
   R: AACTTGCCCTTGCGTAGT
2. Copper-translocating P-type ATPase (4024, 6375)
   F: CTGTCCCAGATCGTTCAGATG
   R: AGGATCGCCGAGAGGATAA
3. CpxP periplasmic heavy metal sensor (8476, 8916)
   F: AAGCGTCCAGCATGTGAT
   R: GACTGTTCGGTGAGGTTCTT
4. CusB efflux RND transporter subunit (13653, 15179)
   F: TGACCTTGCTTGGCATGA
   R: CACCGTGGATGTCGTCTG
5. CopB copper resistance protein (19784, 20860)
   F: GATCGGTCCCTACTTCAATCTTC
   R: CGCTCACCTCAAACCAGTAG
6. CzcD (69328, 69984)
   F: CGCCACACCAGCCTATC
   R: GACCAACACCACGACGAA
7. CzcA heavy metal efflux RND transporter (75025, 78267)
   F: CGAAGGCACTGACCTCTATTT
   R: ATCTGCGGCTGTACTGATG
8. TolC outer membrane efflux protein (85600, 86829)
   F: TTCAGAGCGAGAACATCGG
   R: GCCCAGCTCCAGCTTCT
9. CusA (88533, 91781)
   F: GGTCAACGCCACCATTAAGA
   R: GTTGCCTAGCAGAAGGAAGAG
10. Rho Control CB4 chromosome
   F: GCCGACAAGCGGATCTT
   R: CGCAGCACATAGGTCTTCT

Table B.2. Predicted amino acid sequence identity of the RepC (2a),ParB (2b), and MobA (2c) proteins coded by the large plasmid group.

(A)

RepC	FWC2	FWC26p1	AP07	Ji-3-8	K31p1
FWC2					
FWC26p1	81.36%				
AP07	74.29%	72.86%			
Ji-3-8	74.29%	72.86	94.05%		
K31p1	70.36%	68.03%	74.58%	74.10%	
K31p2	np	np	np	np	np

(B)

ParB	FWC2	FWC26p1	AP07	Ji-3-8	K31p1
FWC2					
FWC26p1	59.78%				
AP07	73.44%	62.01			
Ji-3-8	71.34%	61.86%	82.22%		
K31p1	59.66%	61.38%	61.11%	61.36%	
K31p2	58.17%	57.37%	59.84%	56.60%	57.40%

(C)

MobA	FWC2	FWC26p1	AP07	Ji-3-8	K31p1
FWC2					
FWC26p1	99.30%				
AP07	70.94%	68.81			
Ji-3-8	76.35%	67.20%	76.10%		
K31p1	72.95%	69.62%	82.73%	77.31%	
K31p2	46.38%	48.03%	48.00%	49.33%	47.88%

Table B.3. Predicted amino acid sequence identity of RepB(3a), ParB(3b), and MobA(3c) for the medium plasmid group.

(A)

RepB	Cb4	Root1455	FWC26p2
CB4			
Root1455	94.13%		
FWC26p2	95.60%	96.48%	

(B)

ParB	Cb4	Root1455	FWC26p2
CB4			
Root1455	97.17%		
FWC26p2	89.36%	85.80%	

(C)

MobA	CB4	Root1455	FWC26p2
CB4			
Root1455	96.47%		
FWC26p2	89.94%	92.90%	

Table B.4. Klett readings for addition of $CuSO_4$ to CB4 and NA1000 duringmid-log phase growth.

16um	NAcu1	NAcu2	NAC1	NAC2	CBC1	CBC2	CBcu1	CBcu2
T0	56	55	48	48	32	48	44	47
T1	73	70	71	73	42	61	54	63
T2	75	76	92	89	54	81	67	77
T3	83	81	116	114	76	100	88	99
T4	85	85	141	119	95	117	106	119
Slope	6.8	7.1	23.1	18.3	16	17.7	15.8	18
Average	6.95		20.7		16.85		16.9	
%Growth	0.335749				1.002967			
	34%				100%			

APPENDIX C

CHAPTER 3 SUPPLEMENTARY TABLES

Table C.1. Primers for flanking regions of copper-translocating P-type ATPase CB4 plasmid gene.

Primer	Nucleotide sequence
EcoF1	TTTTTTGAATTCCAATCGACGAGTCTATGGTCAC
ClaR1	TTTTTTATCGATAGGATCGCCGAGAGGATAA
BsmF2	TTTTTTGAATGCGGGTTGACGAAACCGATCTACTC
AvaR2	TTTTTTCCCGAGGGCCTGTTCCACCATGAA